



---

*Research article*

## **A novel asymmetric form of the power half-logistic distribution with statistical inference and real data analysis**

**Amal S. Hassan<sup>1,\*</sup>, Najwan Alsadat<sup>2</sup>, Mohammed Elgarhy<sup>3</sup>, Laxmi Prasad Sapkota<sup>4</sup>, Oluwafemi Samson Balogun<sup>5</sup> and Ahmed M. Gemeay<sup>6</sup>**

<sup>1</sup> Faculty of Graduate Studies for Statistical Research, Cairo University, 5 Dr. Ahmed Zewail Street, Giza 12613, Egypt

<sup>2</sup> Department of Quantitative Analysis, College of Business Administration, King Saud University, P.O. Box 71115, Riyadh 11587, Saudi Arabia

<sup>3</sup> Department of Basic Sciences, Higher Institute of Administrative Sciences, Belbeis, AlSharkia, Egypt

<sup>4</sup> Department of Statistics, Tribhuvan University, Tribhuvan Multiple Campus, Palpa, Nepal

<sup>5</sup> Department of Computing, University of Eastern Finland, FI-70211, Finland

<sup>6</sup> Department of Mathematics, Faculty of Science, Tanta University, Tanta 31527, Egypt

\* **Correspondence:** Email: [amal52\\_soliman@cu.edu.eg](mailto:amal52_soliman@cu.edu.eg)

**Abstract:** This study provided a significant contribution to developing an adaptable trigonometric extension of the power half-logistic distribution. To be more specific, we created an innovative two-parameter lifetime model called the sine power half-logistic distribution (SPHLD) by using features from the sine-generated family of distributions. The novel distribution could be more effective in modeling lifetime phenomena when asymmetric data was presented, which was the primary motivating factor. The SPHLD's density function plots showed that the distribution adopted several asymmetric shape configurations. Furthermore, the SPHLD's hazard rate plots displayed both monotonic increases and decreases. The quantile function, moments, incomplete moment, and stress-strength reliability were among the statistical characteristics of the SPHLD that were computed. Statistical inference using sixteen distinct classical estimating techniques was utilized to estimate the SPHLD parameters. A simulation study was done to evaluate the consistency of the different estimates and determine the best estimating approach based on some accuracy measures. Analyses of real data revealed that the SPHLD performed better than a number of alternative distributions.

**Keywords:** power half logistic distribution; trigonometric distributions; stress-strength reliability; minimum spacing absolute-log distance; Anderson-Darling left tail second order; data analysis

---

## 1. Introduction

### 1.1. An overview of generated families

The features and interrelationships of distribution functions are important for representing naturally occurring events. The conventional distributions, however, have not been able to adequately describe complex data due to the dynamic and ever-increasing complexity of current datasets. Aware of these limitations, scientists have focused their attention on improving the effectiveness and suitability of these distributions in an attempt to find better matches for the variety of real-world information. There are several approaches for defining statistical distributions. Different approaches are available for defining failure rate and density functions to create distributions with more desired and modifiable qualities. One of these approaches is the development of generated families of the probability distributions. Notable has helped to create new distribution families that aim to solve the shortcomings of their earlier versions. Recently, a variety of academics have developed an interest in the families of distributions that have been generated, such as the Marshall Olkin-G proposed by Ref. [1], beta-G presented by Ref. [2], transformed- transformer (T-X) family proposed by Ref. [3], Topp-Leone-G prepared by Ref. [4], new Topp Leone-G prepared by Ref. [5], transmuted odd Fréchet-G created by Ref. [6], modified T-X family prepared by Ref. [7], truncated power Lomax-G proposed by Ref. [8], odd Lindley-G, and power Lindley-G discussed, respectively, by [9, 10]. For more recently generated families, the reader can refer to [11–14].

Nowadays, there has been a lot of interest in the families represented by "trigonometric transformations" due to their versatility and ability for modeling a variety of real-world datasets. The sine-G (S-G) family of distributions, which was first presented by Ref. [15], is the first trigonometric family. The cumulative distribution function (CDF) of the S-G family is as follows:

$$G(t; \zeta) = \sin\left(\frac{1}{2}\pi F(t; \zeta)\right), \quad t \in R, \quad (1.1)$$

where  $F(t; \zeta)$  is the baseline CDF of a continuous distribution and  $\zeta$  is a parameter vector. The following is the probability density function (PDF) associated with CDF (1.1):

$$g(t; \zeta) = \frac{1}{2}\pi f(t; \zeta) \cos\left(\frac{1}{2}\pi F(t; \zeta)\right), \quad t \in R, \quad (1.2)$$

where  $f(t; \zeta)$  is the PDF corresponding to  $F(t; \zeta)$ . As indicated in Ref. [16], the S-G family offers several benefits, such as the following, (i) It is straightforward; (ii) the CDF  $G(t; \zeta)$  and the CDF  $F(t; \zeta)$  have the same number of parameters that is, no extra parameter is used therefore, there is no risk of over-parameterization; (iii) the trigonometric function enables  $G(t; \zeta)$  to expand  $F(t; \zeta)$ 's flexibility, resulting in the creation of new flexible models.

### 1.2. Half logistic distribution & related works

One popular lifespan model that was created by Ref. [17] is the half logistic distribution (HLD). It has attracted significant interest due to its simplicity, tractable mathematical features, and capacity to accommodate survival data. Basically, the HLD is characterized by the survival function (SF) provided

by

$$S(y) = \frac{2}{1 + e^{\delta y}}; \quad y, \delta > 0,$$

where  $\delta > 0$ , is the scale parameter. Recently, a number of HLD generalizations and extensions have been proposed in an effort to increase or use some of its features. Among them are the inverse HLD [18], generalized HLD [19], exponentiated half logistic-G [20], McDonald-HLD [21], type II half logistic-G [22], power- HLD [23], Kumaraswamy-HLD [24], Marshall-Olkin HLD [25], type I half logistic Lindley distribution [26], transmuted-HLD [27], type II half logistic Weibull distribution [28], half-logistic generalized Weibull distribution [29], type I half logistic Burr X-G [30], modified-HLD [31], unit exponentiated-HLD [32], and, for more extended forms, refer to [33–36].

The main focus here is on a more flexible model, the power-HLD (PHLD) with an extra shape parameter compared to HLD. The CDF and PDF, with scale parameter  $\delta > 0$  and shape parameter  $\gamma > 0$  of the PHLD, are provided by:

$$F(t; \zeta) = 1 - \frac{2}{1 + e^{\delta t^\gamma}}; \quad t > 0, \quad (1.3)$$

and

$$f(t; \zeta) = \frac{2\delta\gamma t^{\gamma-1} e^{\delta t^\gamma}}{(1 + e^{\delta t^\gamma})^2}; \quad t > 0, \quad (1.4)$$

where  $\zeta = (\delta, \gamma)$ .

### 1.3. Work motivation

The requirement for flexible and efficient probability distributions is fundamental in statistics and probability theory. The fact that no one distribution fits every dataset makes academics constantly look for ways to improve the accuracy and flexibility of current models. In light of this, a new two-parameter distribution called the sine-PHLD (SPHLD) was created, which is based on the PHLD. The SPHLD is intended to efficiently simulate datasets with a range of asymmetrical shapes. The following motivates us to recommend the SPHLD.

- 1) To enhance the versatility of the traditional PHLD in the modeling of different phenomena. The SPHLD can be used to model skewed data from a range of sources, including agricultural and survival times. Additionally, SPHLD performs better than other distributions that are available in the literature, according to our evaluation of its performance on actual data.
- 2) A few SPHLD features are identified, including the quantile function (QF), moments (both full and incomplete), and stress-strength (SS) reliability.
- 3) To evaluate the SPHLD parameters' behavior, sixteen estimation strategies are advised. The approaches that have been suggested include percentiles (PC), Kolmogorov, maximum product spacing (MPS), ordinary least squares (OLS), Anderson-Darling (AD), Cramér-von Mises (CVM), left tail AD (LTAD), minimum spacing square distance (MSSD), maximum likelihood (ML), weighted LS (WLS), minimum spacing absolute-log distance (MSALD), right-tail AD (RTAD), AD left tail second order (ADSO), minimum spacing Linex distance (MSLND), minimum spacing absolute distance (MSAD), and minimum spacing square log distance (MSSLD).

- 4) A comprehensive simulation study is conducted to evaluate the behaviors of different estimators because it is challenging to compare them theoretically. Tables and graphs were included to demonstrate how these methods worked for different parameter values and sample sizes.
- 5) In comparison to other current models, the SPHLD's adaptability makes it a competitive model for fitting real data. This study illustrates its efficacy by contrasting it with a number of well-known statistical models, such as the exponentiated generalized standard HLD, exponentiated HLD, Poisson generalized HLD, Kumaraswamy HLD, Type-II half logistic Weibull distribution, and PHLD. Two practical applications from the fields of agriculture and medical science further demonstrate the SPHLD's superiority.

This article has the following setup: A novel model extending the PHLD is presented in Section 2. The essential properties of the SPHLD distribution are obtained in Section 3. Many methods for estimating model parameters are covered in Section 4. Section 5 uses Monte Carlo simulations to conduct a numerical analysis. Two real datasets are quantitatively examined in Section 6, and the results are presented in Section 7.

## 2. Description of the model

In this section, a relatively new flexible distribution model known as the SPHLD is created by setting CDF (1.3) into CDF (1.1). This allows us to get the CDF, which may be represented as

$$F(t; \zeta) = \sin \left[ \frac{1}{2} \pi \left( 1 - \frac{2}{1 + e^{\delta t^\gamma}} \right) \right] = \cos \left( \frac{\pi}{1 + e^{\delta t^\gamma}} \right); \quad t, \delta, \gamma > 0, \quad (2.1)$$

where  $\zeta = (\delta, \gamma)$  is the set of parameters. The PDF of the SPHLD associated with (2.1) is given by:

$$f(t; \zeta) = \frac{\delta \gamma \pi t^{\gamma-1} e^{\delta t^\gamma}}{(1 + e^{\delta t^\gamma})^2} \sin \left( \frac{\pi}{1 + e^{\delta t^\gamma}} \right); \quad t, \delta, \gamma > 0. \quad (2.2)$$

For  $\gamma = 1$ , the PDF (2.2) reduces to the sine HLD (SHLD) as a new sub-model. The SF and hazard rate function (HRF) of the SPHLD are as below:

$$S(t; \zeta) = 1 - \cos \left( \frac{\pi}{1 + e^{\delta t^\gamma}} \right), \quad (2.3)$$

and

$$h(t; \zeta) = \frac{\delta \gamma \pi t^{\gamma-1} e^{\delta t^\gamma}}{(1 + e^{\delta t^\gamma})^2} \sin \left( \frac{\pi}{1 + e^{\delta t^\gamma}} \right) \left[ 1 - \cos \left( \frac{\pi}{1 + e^{\delta t^\gamma}} \right) \right]^{-1}.$$

The SPHLD can accurately represent the positively skewed, reverse J-shaped, and unimodal data (left panel in Figure 1) with varying failure rates and decreasing, increasing, and reverse J-shaped failure data (right panel in Figure 1) structures. Figure 2 shows the 3D plots of the PDF and HRF for the SPHLD at  $\delta = 1.5$ .

## 3. Some statistical characteristics

Several statistical features, including SS reliability, inverse moments, QF, and central moments, have been covered in the subsections that follow.

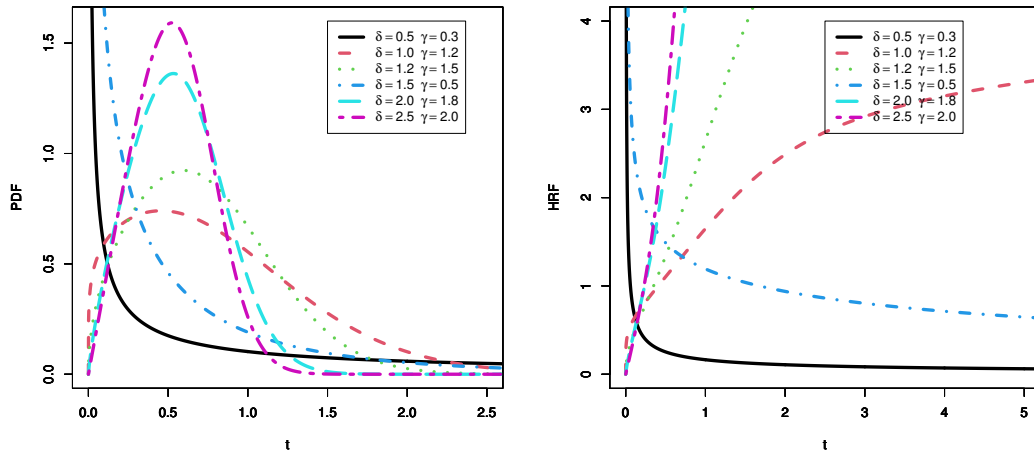


**Figure 1.** Plots of PDF and HRF for the SPHLD.

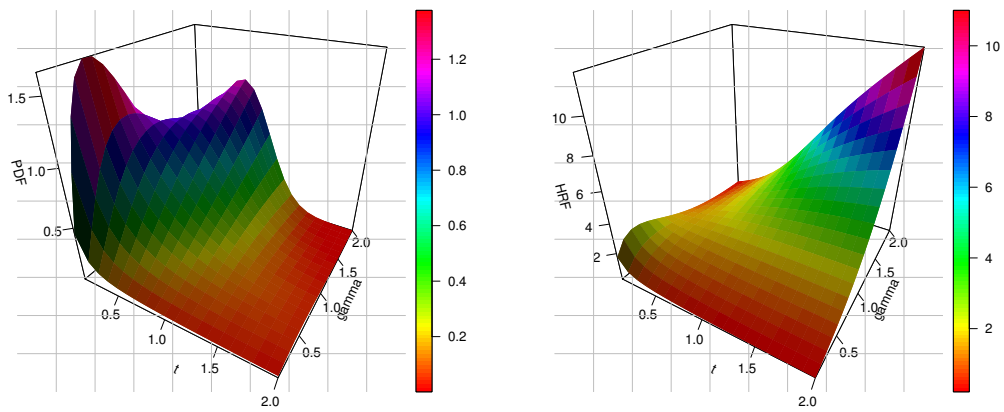


**Figure 2.** The 3D plots of the PDF and HRF for the SPHLD at  $\delta = 1.5$ .

### 3.1. Quantile function

The QF of the SPHLD is determined by inverting (2.1) as follows:

$$Q(p) = \left[ \frac{1}{\delta} \ln \left( \frac{\pi}{\cos^{-1}(p)} - 1 \right) \right]^{1/\gamma}; \quad 0 < p < 1. \quad (3.1)$$

Specifically, by setting  $p = 0.25, 0.5,$  and  $0.75,$  respectively, in (3.1), the first quartile, or  $Q_1,$  the second quartile, or  $Q_2,$  and the third quartile, or  $Q_3,$  are achieved. Some numerical values of the proposed model quantiles are presented in Table 1.

**Table 1.** Some numerical values for the proposed model quantiles.

Parameters		Measures							
$\delta$	$\gamma$	$Q(0.1)$	$Q(0.25)$	$Q(0.35)$	$Q(0.5)$	$Q(0.6)$	$Q(0.75)$	$Q(0.85)$	$Q(0.95)$
0.15	0.5	0.724887	4.68121	9.54363	21.3535	33.6724	64.8572	105.342	212.237
	1.0	0.851403	2.16361	3.08928	4.62098	5.80279	8.0534	10.2636	14.5684
	3.0	0.947789	1.29338	1.45642	1.66563	1.79699	2.00444	2.1732	2.44233
	5.0	0.968338	1.16691	1.25306	1.35815	1.42144	1.51773	1.59316	1.70876
	7.0	0.977281	1.11656	1.17484	1.24441	1.28556	1.34718	1.39467	1.46623
	10	0.984042	1.08023	1.1194	1.1654	1.19224	1.23196	1.26221	1.3072
0.6	0.5	0.0453054	0.292575	0.596477	1.33459	2.10452	4.05357	6.58386	13.2648
	1.0	0.212851	0.540902	0.772319	1.15525	1.4507	2.01335	2.5659	3.64209
	3.0	0.59707	0.814779	0.917485	1.04928	1.13203	1.26272	1.36903	1.53857
	5.0	0.733863	0.884349	0.949641	1.02928	1.07725	1.15023	1.20739	1.295
	7.0	0.801698	0.915955	0.963765	1.02083	1.05459	1.10514	1.1441	1.2028
	10	0.856658	0.940398	0.974495	1.01454	1.03791	1.07249	1.09881	1.13798
0.9	0.5	0.0201357	0.130033	0.265101	0.593152	0.935344	1.80159	2.92616	5.89547
	1.0	0.1419	0.360602	0.514879	0.770164	0.967132	1.34223	1.7106	2.42806
	3.0	0.521588	0.711775	0.801497	0.916631	0.988922	1.10309	1.19596	1.34406
	5.0	0.676701	0.815465	0.875671	0.94911	0.993338	1.06063	1.11335	1.19413
	7.0	0.75658	0.864407	0.909526	0.96338	0.995237	1.04294	1.07971	1.13511
	10	0.822618	0.903031	0.935773	0.974223	0.996664	1.02987	1.05515	1.09276
1.5	0.5	0.00724887	0.0468121	0.0954363	0.213535	0.336724	0.648572	1.05342	2.12237
	1.0	0.0851403	0.216361	0.308928	0.462098	0.580279	0.80534	1.02636	1.45684
	3.0	0.439925	0.600334	0.676009	0.773116	0.834089	0.930379	1.00871	1.13363
	5.0	0.61098	0.736268	0.790626	0.856933	0.896866	0.957626	1.00522	1.07816
	7.0	0.703335	0.803573	0.845517	0.895581	0.925196	0.969546	1.00372	1.05522
	10	0.781652	0.85806	0.889172	0.925707	0.94703	0.978584	1.00261	1.03834
2.5	0.5	0.00260959	0.0168523	0.0343571	0.0768725	0.121221	0.233486	0.37923	0.764053
	1.0	0.0510842	0.129817	0.185357	0.277259	0.348167	0.483204	0.615817	0.874101
	3.0	0.371047	0.506341	0.570168	0.652071	0.703498	0.784712	0.85078	0.956138
	5.0	0.551642	0.664762	0.713841	0.773708	0.809762	0.864622	0.907591	0.973447
	7.0	0.653837	0.747021	0.786013	0.832554	0.860085	0.901313	0.933086	0.980961
	10	0.742726	0.815329	0.844891	0.879607	0.899868	0.92985	0.952676	0.986634
4.5	0.5	0.00080543	0.00520134	0.010604	0.0237261	0.0374137	0.0720635	0.117046	0.235819
	1.0	0.0283801	0.0721203	0.102976	0.154033	0.193426	0.268447	0.34212	0.485612
	3.0	0.305027	0.416248	0.468718	0.536049	0.578325	0.645088	0.699401	0.786013
	5.0	0.490459	0.591033	0.634669	0.687896	0.719951	0.768726	0.80693	0.865482
	7.0	0.601176	0.686855	0.722707	0.765499	0.790813	0.828721	0.857935	0.901954
	10	0.700328	0.768787	0.796661	0.829395	0.848499	0.87677	0.898293	0.930313

### 3.2. Moments

Studying the random variable's moments can help in understanding a number of its distribution characteristics. We'll provide the  $n$ th moment of the recommended SPHLD below.

$$E(T^n) = \int_0^{\infty} t^n \frac{\delta\gamma\pi t^{\gamma-1} e^{\delta t^\gamma}}{(1 + e^{\delta t^\gamma})^2} \sin\left(\frac{\pi}{1 + e^{\delta t^\gamma}}\right) dt. \quad (3.2)$$

The following is the series of the sine function:

$$\sin(t) = \sum_{j=0}^{\infty} \frac{(-1)^j t^{2j+1}}{(2j+1)!}. \quad (3.3)$$

Using expansion (3.3) in (3.2) gives

$$E(T^n) = \sum_{j=0}^{\infty} \frac{(-1)^j \pi^{2j+2}}{(2j+1)!} \int_0^{\infty} \frac{\delta\gamma t^{n+\gamma-1} e^{-2(j+1)\delta t^\gamma}}{(1 + e^{-\delta t^\gamma})^{2j+3}} dt. \quad (3.4)$$

The following is the binomial expansion

$$(1 + y)^{-(a+1)} = \sum_{i=0}^{\infty} (-1)^i \binom{a+i}{i} y^i. \quad (3.5)$$

Employing (3.5) in (3.4), we have

$$E(T^n) = \sum_{j,i=0}^{\infty} \frac{\eta_{i,j} \delta^{-(n/\gamma)}}{(2(j+1) + i)^{(n/\gamma)+1}} \Gamma\left(\frac{n}{\gamma} + 1\right),$$

where  $\eta_{i,j} = \frac{(-1)^{j+i} \pi^{2j+2}}{(2j+1)!} \binom{2j+2+i}{i}$ ,  $\Gamma(\cdot)$  is the gamma function (GaF).

Furthermore, using moments around the origin, we may compute the  $n$ th central moment of  $T$  based on the complete moments as follows:

$$\mu_n = E[(T - E(T))^n] = \sum_{k=0}^n (-1)^k \binom{n}{k} (E(T))^k (E(T))^{n-k}.$$

Next, we get skewness coefficient  $SK = \mu_3/\mu_2^{1.5}$  and kurtosis coefficient  $KU = \mu_4/\mu_2^2$ . They are essential for determining whether the SPHLD is symmetrical or asymmetric. In conclusion, Figure 3 offers 3D plots of mean, variance, skewness, and kurtosis for the SPHLD.

The  $n$ th incomplete moment (IM) of the SPHLD is obtained by using PDF (2.2) as follows:

$$\vartheta_n(z) = \int_0^z t^n \frac{\delta\gamma\pi t^{\gamma-1} e^{\delta t^\gamma}}{(1 + e^{\delta t^\gamma})^2} \sin\left(\frac{\pi}{1 + e^{\delta t^\gamma}}\right) dt.$$

Using the expansions (3.2) and (3.4), we have

$$\begin{aligned} \vartheta_n(z) &= \sum_{j,i=0}^{\infty} \eta_{i,j} \int_0^z \delta\gamma t^{n+\gamma-1} e^{-(2(j+1)+i)\delta t^\gamma} dt \\ &= \sum_{j,i=0}^{\infty} \frac{\eta_{i,j} \delta^{-(n/\gamma)}}{((2(j+1)+i)^{(n/\gamma)+1})} \Gamma\left(\frac{n}{\gamma} + 1, (2(j+1) + i)\delta z^\gamma\right), \end{aligned}$$

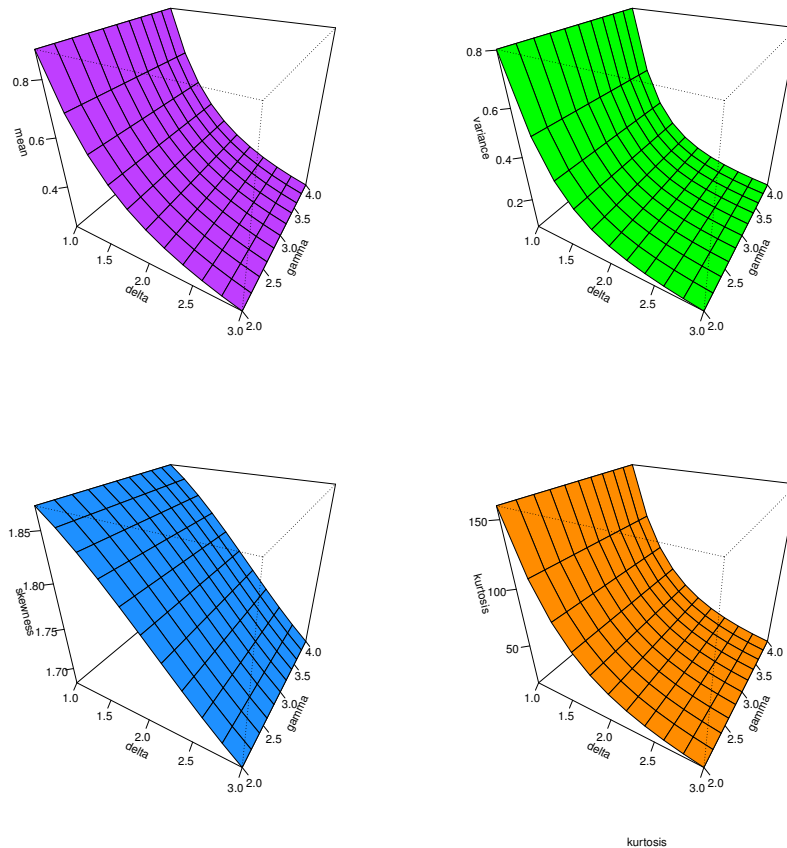


**Figure 3.** The 3D plots of mean, variance, skewness and kurtosis for the SPHLD.

where  $\Gamma(\cdot, x)$  is the incomplete GaF. A valuable tool in science, engineering, economics, and demography, the IM is used to estimate Lorenz and Bonferroni curves. These values may be mathematically defined as  $L(z) = \vartheta_1(z)/E(T)$  and  $B(z) = \vartheta_1(z)/pE(T)$ . Additionally, it is employed in determining the mean waiting time, say  $MW(z) = z - \vartheta_1(z)/F(z; \zeta)$ , and the mean residual life, say  $MR(z) = [1 - \vartheta_1(z)]/S(z; \zeta) - z$ .

### 3.3. Stress-strength reliability

The life of a component with random strength  $T_1$  under random stress  $T_2$  is described by the SS model. When the component is subjected to stress greater than its strength, it fails instantly, and when  $T_1 > T_2$ , it works properly. Suppose that  $T_1 \sim SPHLD(\delta_1, \gamma)$  and  $T_2 \sim SPHLD(\delta_2, \gamma)$ , then the SS reliability is given by

$$\beta = P(T_2 < T_1) = \int_0^\infty \frac{\delta_1 \gamma \pi t^{\gamma-1} e^{\delta_1 t^\gamma}}{(1 + e^{\delta_1 t^\gamma})^2} \sin\left(\frac{\pi}{1 + e^{\delta_1 t^\gamma}}\right) \cos\left(\frac{\pi}{1 + e^{\delta_2 t^\gamma}}\right) dt, \quad (3.6)$$

since

$$\cos(t) = \sum_{j_2=0}^{\infty} \frac{(-1)^{j_2} t^{2j_2}}{2^{j_2} j_2!}. \quad (3.7)$$



Then, using expansions (3.3) and (3.7) in (3.6) provide

$$\beta = \sum_{j_1, j_2=0}^{\infty} D_{j_1, j_2} \int_0^{\infty} \frac{\delta_1 \gamma t^{\gamma-1} e^{-2(j_1+1)\delta_1 t^\gamma}}{(1 + e^{-\delta_1 t^\gamma})^{2j_1+3}} \frac{e^{-2\delta_2 j_2 t^\gamma}}{(1 + e^{-\delta_2 t^\gamma})^{2j_2}} dt, \quad (3.8)$$

where  $D_{j_1, j_2} = \frac{(-1)^{j_1+j_2} \pi^{2j_1+2j_2+2}}{(2j_1+1)! 2j_2!}$ . Again, using the expansion (3.5) two times in (3.8), we obtain

$$\beta = \sum_{j_1, j_2, i_1, i_2=0}^{\infty} D_{j_1, j_2} K_{i_1, i_2} \int_0^{\infty} \delta_1 \gamma t^{\gamma-1} e^{-\{\delta_1 [2(j_1+1)+i_1] + \delta_2 (i_2+2j_2)\} t^\gamma} dt, \quad (3.9)$$

where  $K_{i_1, i_2} = (-1)^{i_1+i_2} \binom{2j_1+2+i_1}{i_1} \binom{2j_2-1+i_2}{i_2}$ . Hence, (3.9) has the following expression

$$\beta = \sum_{j_1, j_2, i_1, i_2=0}^{\infty} \frac{D_{j_1, j_2} K_{i_1, i_2} \delta_1}{[\delta_1 [2(j_1+1)+i_1] + \delta_2 (i_2+2j_2)]}.$$

#### 4. Estimation methods

To estimate the SPHLD parameters, we investigate various classical estimation techniques in this section. The proposed methods are AD, MSALD, MPS, ML, Kolmogorov, LTAD, MSAD, CVM, OLS, MSSD, PC, WLS, MSLD, RTAD, ADSO, and MSSLD. In order to enhance the straightforward nature of the estimation techniques, we have incorporated a more comprehensive explanation of the derivation process for every equation.

##### 4.1. Maximum likelihood estimation

The SPHLD parameters are estimated in this subsection using the ML technique. Let  $t_1, t_2, \dots, t_n$  be an  $n$  observed sample from PDF (2.2). The log-likelihood function is as below:

$$\log \ell \propto n \log(\delta \gamma) + \sum_{i=1}^n (\gamma - 1) \log t_i + \sum_{i=1}^n \delta t_i^\gamma - 2 \sum_{i=1}^n \log(1 + e^{\delta t_i^\gamma}) + \sum_{i=1}^n \log \left[ \sin \left( \frac{\pi}{1 + e^{\delta t_i^\gamma}} \right) \right].$$

The log-likelihood function can be maximized to determine the ML estimators (MLEs)  $\hat{\delta}_1$  and  $\hat{\gamma}_1$  of the parameters  $\delta$  and  $\gamma$ . Alternatively, the following differential equations can be solved about of  $\delta$  and  $\gamma$

$$\frac{\partial \log \ell}{\partial \delta} = \frac{n}{\delta} + \sum_{i=1}^n t_i^\gamma - 2 \sum_{i=1}^n \frac{t_i^\gamma}{1 + e^{-\delta t_i^\gamma}} - \sum_{i=1}^n \frac{\pi t_i^\gamma}{(1 + e^{-\delta t_i^\gamma})^2} \cot \left( \frac{\pi}{1 + e^{\delta t_i^\gamma}} \right) = 0, \quad (4.1)$$

and

$$\frac{\partial \log \ell}{\partial \gamma} = \frac{n}{\gamma} + \sum_{i=1}^n \log t_i + \sum_{i=1}^n \delta t_i^\gamma \log t_i - 2 \sum_{i=1}^n \frac{\delta t_i^\gamma \log t_i}{(1 + e^{-\delta t_i^\gamma})} - \sum_{i=1}^n \cot \left( \frac{\pi}{1 + e^{\delta t_i^\gamma}} \right) \frac{\delta \pi t_i^\gamma \log t_i}{(1 + e^{-\delta t_i^\gamma})^2} = 0. \quad (4.2)$$

Since the aforementioned Eqs (4.1) and (4.2) have no explicit solutions, in order to determine the MLEs of the SPHLD parameters, nonlinear numerical techniques must be used.

#### 4.2. Anderson-darling methods

A particular class of minimal distance estimators is the AD estimators. Here, four different estimators for the SPHLD parameters based on the AD approach are determined. These estimators are AD estimators (ADEs), RTAD estimators (RTADEs), ADSO estimators (ADSOEs), and LTAD estimators (LTADEs).

Suppose that  $t_{(1)}, t_{(2)}, \dots, t_{(n)}$  are the order statistics of a random sample drawn from the SPHLD. Minimizing the following function with respect to the SPHLD parameters, the ADEs  $\hat{\delta}_2$  and  $\hat{\gamma}_2$  of  $\delta$  and  $\gamma$  are determined

$$A_1(\zeta) = -n - \frac{1}{n} \sum_{b=1}^n (2b-1) \{ \log F(t_{(b)} | \zeta) + \log (S(t_{(n-b+1)} | \zeta)) \},$$

where  $F(\cdot)$  is the CDF (2.1) and  $S(\cdot)$  is the SF (2.3). Solving the following nonlinear equations will also yield the ADEs:

$$\sum_{b=1}^n (2b-1) \left\{ \frac{v_\zeta(t_{(b)} | \zeta)}{F(t_{(b)} | \zeta)} - \frac{v_\zeta(t_{(n-b+1)} | \zeta)}{S(t_{(n-b+1)} | \zeta)} \right\} = 0, \quad \zeta = (\delta, \gamma),$$

where

$$v_\delta(t_{(b)} | \zeta) = \frac{\partial F(t_{(b)} | \zeta)}{\partial \delta} = \frac{\pi t_{(b)}^\gamma e^{\delta t_{(b)}^\gamma}}{(1 + e^{\delta t_{(b)}^\gamma})^2} \sin\left(\frac{\pi}{1 + e^{\delta t_{(b)}^\gamma}}\right), \quad (4.3)$$

and

$$v_\gamma(t_{(b)} | \zeta) = \frac{\partial F(t_{(b)} | \zeta)}{\partial \gamma} = \frac{\pi t_{(b)}^\gamma \log t_{(b)} e^{\delta t_{(b)}^\gamma}}{(1 + e^{\delta t_{(b)}^\gamma})^2} \sin\left(\frac{\pi}{1 + e^{\delta t_{(b)}^\gamma}}\right). \quad (4.4)$$

The RTADEs  $\hat{\delta}_3$  and  $\hat{\gamma}_3$  of parameters  $\delta$  and  $\gamma$  are determined by minimizing the following function with respect to parameters,

$$A_2(\zeta) = \frac{n}{2} - 2 \sum_{b=1}^n F(t_{(b)} | \delta, \gamma) - \frac{1}{n} \sum_{b=1}^n (2b-1) \log S(t_{(n+1-b)} | \delta, \gamma) = 0, \quad (4.5)$$

where  $F(\cdot)$  is the CDF (2.1) and  $S(\cdot)$  is the SF (2.3). As an alternative to (4.5), the RTADEs can additionally be obtained by solving the following nonlinear equations:

$$-2 \sum_{b=1}^n v_\zeta(t_{(b)} | \delta, \gamma) + \frac{1}{n} \sum_{b=1}^n \frac{(2b-1)}{S(t_{(n+1-b)} | \delta, \gamma)} = 0, \quad \zeta = (\delta, \gamma),$$

where,  $v_\zeta(t_{(b)} | \delta, \gamma)$  and  $\zeta = (\delta, \gamma)$  are given in (4.3) and (4.4).

Next, the ADSOE  $\hat{\delta}_4$  and  $\hat{\gamma}_4$  of parameters  $\delta$  and  $\gamma$  may be obtained by minimizing the function shown below:

$$A_3(\zeta) = 2 \sum_{b=1}^n \log F(t_{(b)} | \delta, \gamma) + \frac{1}{n} \sum_{b=1}^n \frac{2b-1}{F(t_{(b)} | \delta, \gamma)}, \quad (4.6)$$

where  $F(\cdot)$  is the CDF (2.1). The ADSOEs can also be produced by solving the following nonlinear equations as an alternative to Eq (4.6):

$$2 \sum_{b=1}^n \frac{v_{\zeta}(t_{(b)}|\delta, \gamma)}{F(t_{(b)}|\delta, \gamma)} - \frac{1}{n} \sum_{b=1}^n \frac{(2b-1)v_{\zeta}(t_{(b)}|\delta, \gamma)}{[F(t_{(b)}|\delta, \gamma)]^2} = 0, \quad \zeta = (\delta, \gamma),$$

where,  $v_{\zeta}(t_{(b)}|\delta, \gamma)$  and  $\zeta = (\delta, \gamma)$  are given in (4.3) and (4.4).

The LTADE  $\hat{\delta}_5$  and  $\hat{\gamma}_5$  of parameters  $\delta$  and  $\gamma$  are determined, respectively, by minimizing the following function:

$$A_4(\zeta) = \frac{-3n}{2} + 2 \sum_{b=1}^n F(t_{(b)}|\zeta) - \frac{1}{n} \sum_{b=1}^n (2b-1) \log F(t_{(b)}|\zeta). \quad (4.7)$$

The following nonlinear equations can be quantitatively solved in place of (4.7) to get  $\hat{\delta}_5$  and  $\hat{\gamma}_5$  respectively:

$$2 \sum_{b=1}^n F(t_{(b)}|\zeta) v_{\zeta}(t_{(b)}|\delta, \gamma) - \frac{1}{n} \sum_{b=1}^n \frac{(2b-1)}{F(t_{(b)}|\zeta)} v_{\zeta}(t_{(b)}|\delta, \gamma) = 0, \quad \zeta = (\delta, \gamma),$$

where,  $v_{\zeta}(t_{(b)}|\delta, \gamma)$  and  $\zeta = (\delta, \gamma)$  are given in (4.3) and (4.4).

### 4.3. Maximum product spacing

In place of MLE for estimating the unknown parameters of continuous univariate distributions, [37, 38] presented the MPS approach. Ranney [39] demonstrated that in some circumstances, the MPSE asymptotically has the same properties as the MLE and that the MSP method produces consistent estimates while the ML method does not. Let  $t_{(1)}, t_{(2)}, \dots, t_{(n)}$  be the order statistics of a random sample drawn from the SPHLD. Subsequently, the uniform spacing is established by

$$\omega_b(t; \delta, \gamma) = F(t_{(b)}|\delta, \gamma) - F(t_{(b-1)}|\delta, \gamma), \quad b = 1, 2, \dots, n+1,$$

where  $F(t_{(0)}|\delta, \gamma) = 0$ ,  $F(t_{(n+1)}|\delta, \gamma) = 1$ , and  $\sum_{b=1}^{n+1} \omega_b(t; \delta, \gamma) = 1$ . Hence, the following function is maximized with respect to  $\delta$  and  $\gamma$  to obtain the MPS estimators (MPSEs) of the SPHLD.

$$D^{\bullet}(\zeta) = \frac{1}{n+1} \sum_{b=1}^{n+1} \log[\omega_b(t; \delta, \gamma)]. \quad (4.8)$$

It is also possible for assessing the MPSEs  $\hat{\delta}_6$  and  $\hat{\gamma}_6$  of parameters  $\delta$  and  $\gamma$  by solving the following nonlinear equation.

$$\frac{1}{n+1} \sum_{b=1}^{n+1} \frac{v_{\zeta}(t_{(b)}|\zeta) - v_{\zeta}(t_{(b-1)}|\zeta)}{\omega_b(t; \zeta)} = 0,$$

where,  $v_{\zeta}(t_{(b)}|\zeta)$  and  $\zeta = (\delta, \gamma)$  are given in (4.3) and (4.4).

#### 4.4. Ordinary and weighted least-squares

On minimizing the subsequent functions to  $\delta$  and  $\gamma$ , the OLS estimators (OLSEs) and WLS estimators (WLSEs) of the unknown parameters  $\delta$  and  $\gamma$  of the SPHLD distribution are obtained

$$\left. \begin{aligned} ls^{\bullet} &= \sum_{b=1}^n \left( F(t_{(b)}|\zeta) - \frac{b}{n+1} \right)^2 \\ ws^{\bullet} &= \sum_{b=1}^n \frac{(n+1)^2(n+2)}{b(n-b+1)} \left( F(t_{(b)}|\zeta) - \frac{b}{n+1} \right)^2 \end{aligned} \right\}, \quad (4.9)$$

where  $F(\cdot)$  is the CDF (2.1). In an equivalent manner to (4.9), the OLSEs  $\hat{\delta}_7$  and  $\hat{\gamma}_7$  and WLSEs  $\hat{\delta}_8$  and  $\hat{\gamma}_8$  of unknown parameters  $\delta$  and  $\gamma$  may be acquired by working out the following equations, with respect to  $\delta$  and  $\gamma$  :

$$\begin{aligned} \sum_{b=1}^n \left( F(t_{(b)}|\zeta) - \frac{b}{n+1} \right) v_{\zeta}(t_{(b)}|\zeta) &= 0, \\ \sum_{b=1}^n \frac{(n+1)^2(n+2)}{b(n-b+1)} \left( F(t_{(b)}|\zeta) - \frac{b}{n+1} \right) v_{\zeta}(t_{(b)}|\zeta) &= 0, \end{aligned}$$

where  $F(\cdot)$  is the CDF (2.1), and  $v_{\zeta}(t_{(b)}|\delta, \gamma)$  and  $\zeta = (\delta, \gamma)$  are given in (4.3) and (4.4).

#### 4.5. Minimum product spacing distance

Here, the MSSD estimators (MSSDEs), MSLND estimators (MSLNDEs), MSALD estimators (MSALDEs), MSAD estimators (MSADEs), and MSSLD estimators (MSSLDEs) are obtained.

The next function is minimized to obtain the MSSDEs  $\hat{\delta}_9$  and  $\hat{\gamma}_9$  of the SPHLD parameters  $\delta$  and  $\gamma$  :

$$V_1(\zeta) = \sum_{b=1}^{n+1} \left( \omega_b(t; \zeta) - \frac{1}{n+1} \right)^2,$$

where  $\omega_b(t; \zeta) = F(t_{(b)}|\delta, \gamma) - F(t_{(b-1)}|\delta, \gamma)$ . The MSSDEs  $\hat{\delta}_9$  and  $\hat{\gamma}_9$  are generated by solving the following nonlinear equations:

$$\sum_{b=1}^{n+1} \left( \omega_b(t; \zeta) - \frac{1}{n+1} \right) \left[ v_{\zeta}(t_{(b)}|\zeta) - v_{\zeta}(t_{(b-1)}|\zeta) \right] = 0,$$

where  $v_{\zeta}(\cdot|\zeta)$  and  $\zeta = (\delta, \gamma)$  are given in (4.3) and (4.4).

The function that follows is minimized to provide the MSLNDEs  $\hat{\delta}_{10}$  and  $\hat{\gamma}_{10}$  of the SPHLD parameters  $\delta$  and  $\gamma$

$$V_2(\zeta) = \sum_{b=1}^{n+1} \left( e^{\omega_b - \frac{1}{n+1}} - \left( \omega_b - \frac{1}{n+1} \right) - 1 \right)^2. \quad (4.10)$$

The following nonlinear equation can be solved as an alternative to (4.10), in order to find the MSLNDEs  $\hat{\delta}_{10}$  and  $\hat{\gamma}_{10}$

$$\sum_{b=1}^{n+1} \left( e^{\omega_b - \frac{1}{n+1}} - \left( \omega_b - \frac{1}{n+1} \right) - 1 \right) \left( e^{\omega_b - \frac{1}{n+1}} - 1 \right) \left[ v_{\zeta}(t_{(b)}|\delta, \gamma) - v_{\zeta}(t_{(b-1)}|\delta, \gamma) \right] = 0, \quad \zeta = (\delta, \gamma),$$

where,  $v_\zeta(\cdot|\zeta)$  and  $\zeta = (\delta, \gamma)$  are given in (4.3) and (4.4).

Minimizing the function below yields the MSALDEs  $\hat{\delta}_{11}$  and  $\hat{\gamma}_{11}$  of  $\delta$  and  $\gamma$

$$V_3(\zeta) = \sum_{b=1}^{n+1} \left| \log \omega_b(t; \zeta) - \log \frac{1}{n+1} \right|.$$

The MSALDEs  $\hat{\delta}_{11}$  and  $\hat{\gamma}_{11}$  are determined by solving the following nonlinear equations:

$$\sum_{b=1}^{n+1} \frac{\log \omega_b(t; \zeta) - \log \frac{1}{n+1}}{\left| \log \omega_b(t; \zeta) - \log \frac{1}{n+1} \right|} \left[ v_\zeta(t_{(b)}|\zeta) - v_\zeta(t_{(b-1)}|\zeta) \right] \frac{1}{\omega_b(t; \zeta)} = 0,$$

where  $v_\zeta(\cdot|\zeta)$  and  $\zeta = (\delta, \gamma)$  are given in (4.3) and (4.4).

The MSADEs  $\hat{\delta}_{12}$  and  $\hat{\gamma}_{12}$  of the SPHLD parameters  $\delta$  and  $\gamma$  are produced by minimizing the following function:

$$V_4(\zeta) = \sum_{b=1}^{n+1} \left| \omega_b(t; \zeta) - \frac{1}{n+1} \right|.$$

After minimizing the function shown below, the MSADEs  $\hat{\delta}_{12}$  and  $\hat{\gamma}_{12}$  are established

$$\sum_{b=1}^{n+1} \frac{\omega_b(t; \zeta) - \frac{1}{n+1}}{\left| \omega_b(t; \zeta) - \frac{1}{n+1} \right|} \left[ v_\zeta(t_{(b)}|\zeta) - v_\zeta(t_{(b-1)}|\zeta) \right] = 0,$$

where  $v_\zeta(\cdot|\zeta)$  and  $\zeta = (\delta, \gamma)$  are given in (4.3) and (4.4).

The MSSLDEs  $\hat{\delta}_{13}$  and  $\hat{\gamma}_{13}$  of parameters  $\delta$  and  $\gamma$  are produced by minimizing the following function:

$$V_5(\zeta) = \sum_{b=1}^{n+1} \left( \log \omega_b(t; \zeta) - \log \frac{1}{n+1} \right)^2. \quad (4.11)$$

As opposed to using (4.11), the following nonlinear equation must be solved in order to derive the MSSLDEs  $\hat{\delta}_{13}$  and  $\hat{\gamma}_{13}$  :

$$\sum_{b=1}^{n+1} \left( \log \omega_b(t; \zeta) - \log \frac{1}{n+1} \right) \left[ v_\zeta(t_{(b)}|\zeta) - v_\zeta(t_{(b-1)}|\zeta) \right] \frac{1}{\omega_b(t; \zeta)} = 0,$$

where  $v_\zeta(\cdot|\zeta)$  and  $\zeta = (\delta, \gamma)$  are given in (4.3) and (4.4).

#### 4.6. Cramér-von mises

In comparison to other estimators of the same kind, the CVM estimators (CVMEs) are less biased and fall within the category of minimal distance estimators. Finding the difference between the estimated and empirical CDFs allows one to generate these estimators. The function below can be minimized with regard to  $\delta$  and  $\gamma$  to get the CVMEs  $\hat{\delta}_{14}$  and  $\hat{\gamma}_{14}$  of  $\delta$  and  $\gamma$

$$C(\zeta) = \frac{1}{12n} + \sum_{b=1}^n \left\{ F(t_{(b)}|\zeta) - \frac{2b-1}{2n} \right\}^2. \quad (4.12)$$

The following nonlinear equation might be solved in place of (4.12), yielding  $\hat{\delta}_{14}$  and  $\hat{\gamma}_{14}$

$$\sum_{b=1}^n \left\{ F(t_{(b)}|\zeta) - \frac{2b-1}{2n} \right\} v_{\zeta}(t_{(b)}|\zeta) = 0,$$

where  $v_{\zeta}(\cdot|\delta, \gamma)$  and  $\zeta = (\delta, \gamma)$  are given in (4.3) and (4.4).

#### 4.7. Other estimators

In this subsection, the Kolmogorov estimators (KEs) and the PC estimators (PCEs) of the SPHLD parameters are obtained.

The estimation of the SPHLD parameters  $\delta$  and  $\gamma$  is done using the Kolmogorov method. The KEs  $\hat{\delta}_{15}$  and  $\hat{\gamma}_{15}$  are obtained after minimizing the following function:

$$H(\zeta) = \text{Max}_{1 \leq b \leq n} \sum_{b=1}^n \left[ \frac{b}{n} - F(t_{(b)}|\zeta), F(t_{(b)}|\zeta) - \frac{b-1}{n} \right]^2,$$

where  $F(\cdot)$  is the CDF (2.1).

Next, by equating the sample and population percentile values, the PCEs  $\hat{\delta}_{16}$  and  $\hat{\gamma}_{16}$  of the unknown parameters  $\delta$  and  $\gamma$  are produced. The following function can be minimized in relation to  $\delta$  and  $\gamma$  to get the  $\hat{\delta}_{16}$  and  $\hat{\gamma}_{16}$

$$P = \sum_{b=1}^n \left[ z_{(b)} - F^{-1}(p_b) \right]^2, \quad p_b = \frac{b}{n+1}.$$

## 5. Numerical simulation

Using a significant quantity of simulated data, this section compares the performance of several estimate methods for estimating the parameters of the proposed model. In our simulation, we used the suggested model quantity function to create random datasets for a variety of sample sizes ( $n = 25, 75, 150, 200, 250,$  and  $400$ ). In this part, we will investigate the performance and behavior of our model estimators. Furthermore, we will examine the performance of various estimating strategies using a range of metrics, such as average of bias ( $|Bias(\zeta)| = \frac{1}{L} \sum_{i=1}^L |\hat{\zeta} - \zeta|$ ), mean squared errors ( $MSE = \frac{1}{L} \sum_{i=1}^L (\hat{\zeta} - \zeta)^2$ ), mean relative errors ( $MRE = \frac{1}{L} \sum_{i=1}^L |\hat{\zeta} - \zeta|/\zeta$ ), average absolute difference ( $D_{abs} = \frac{1}{nL} \sum_{i=1}^L \sum_{j=1}^n |F(t_{ij}|\zeta) - F(t_{ij}|\hat{\zeta})|$ ), maximum absolute difference ( $D_{max} = \frac{1}{L} \sum_{i=1}^L \max_j |F(t_{ij}|\zeta) - F(t_{ij}|\hat{\zeta})|$ ), and average squared absolute error ( $ASAE = \frac{1}{n} \sum_{i=1}^n \frac{|t_i - \hat{t}_i|}{t_n - t_1}$ ), where the observations  $t_i$  are in ascending order and  $\zeta = (\delta, \gamma)$ .

Tables 6–10 illustrate the results of simulating the specified model parameters using 16 estimating approaches. Figures 4 through 9 visually show the data from Table 6. It is critical to note that all of the parameter estimates for the proposed distribution are quite trustworthy and reasonably near to their real values. As  $n$  increases, all anticipated metrics for each scenario under consideration decline. All of the estimating approaches are quite effective at approximating the recommended model parameters. Table 11 shows that the MPS estimate has the lowest overall score, equal to 67.0 for the criteria included in

our investigation, followed by the ML estimate as the second-best method for our investigation with a score of 69.0. Table 11 displays the total rankings for all estimating procedures.

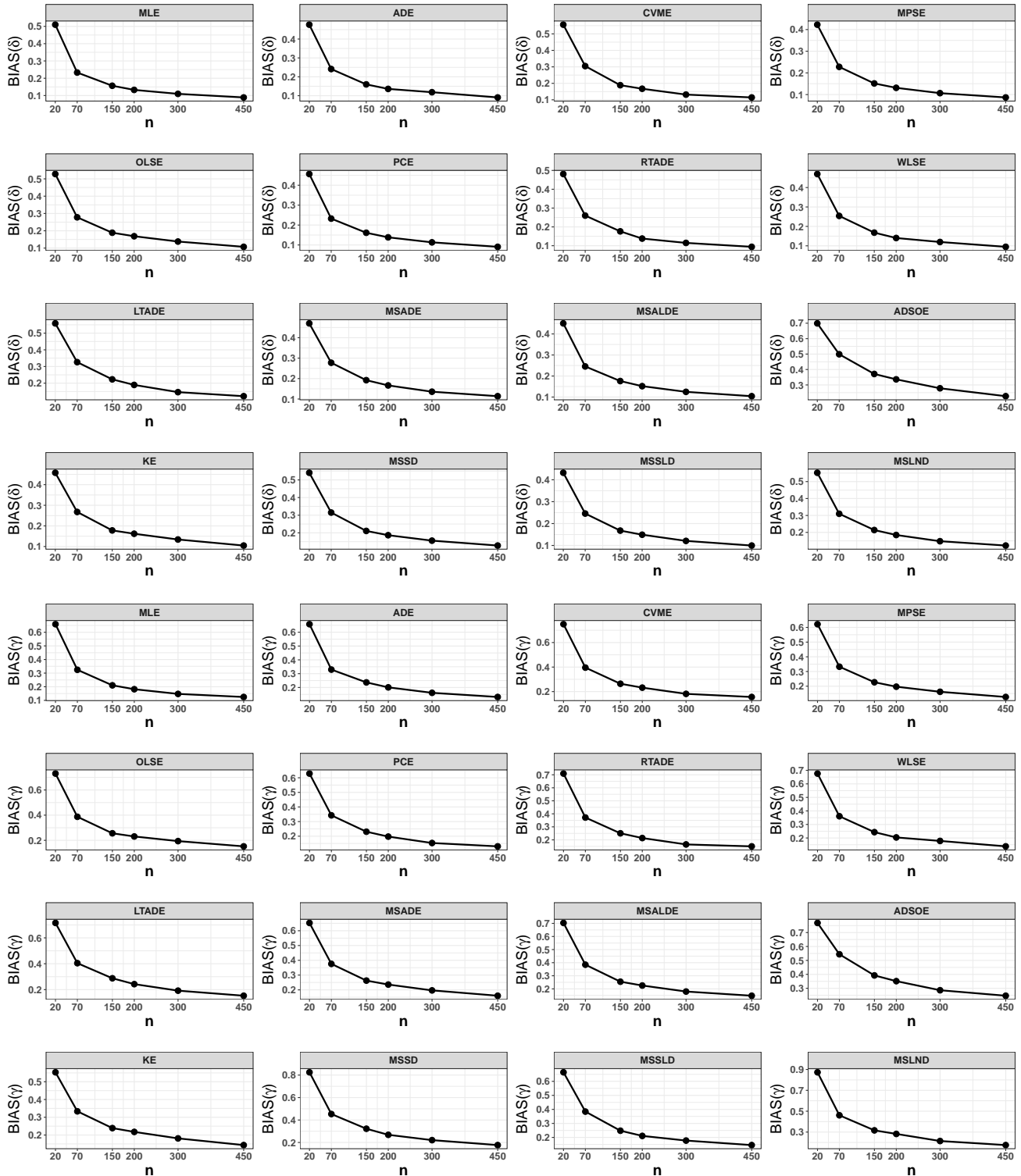


Figure 4. Graphical representation for BIAS values presented in Table 6.

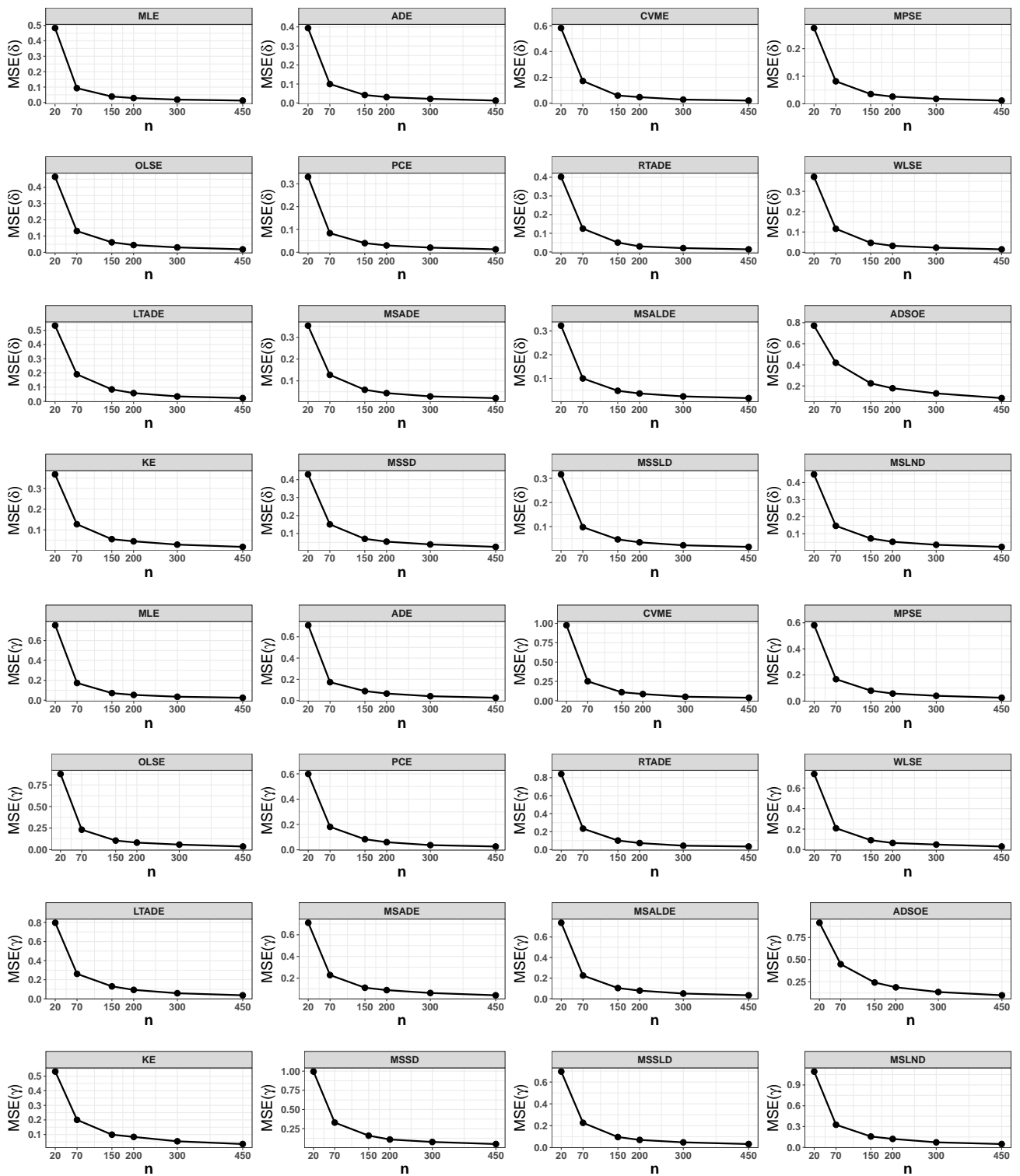
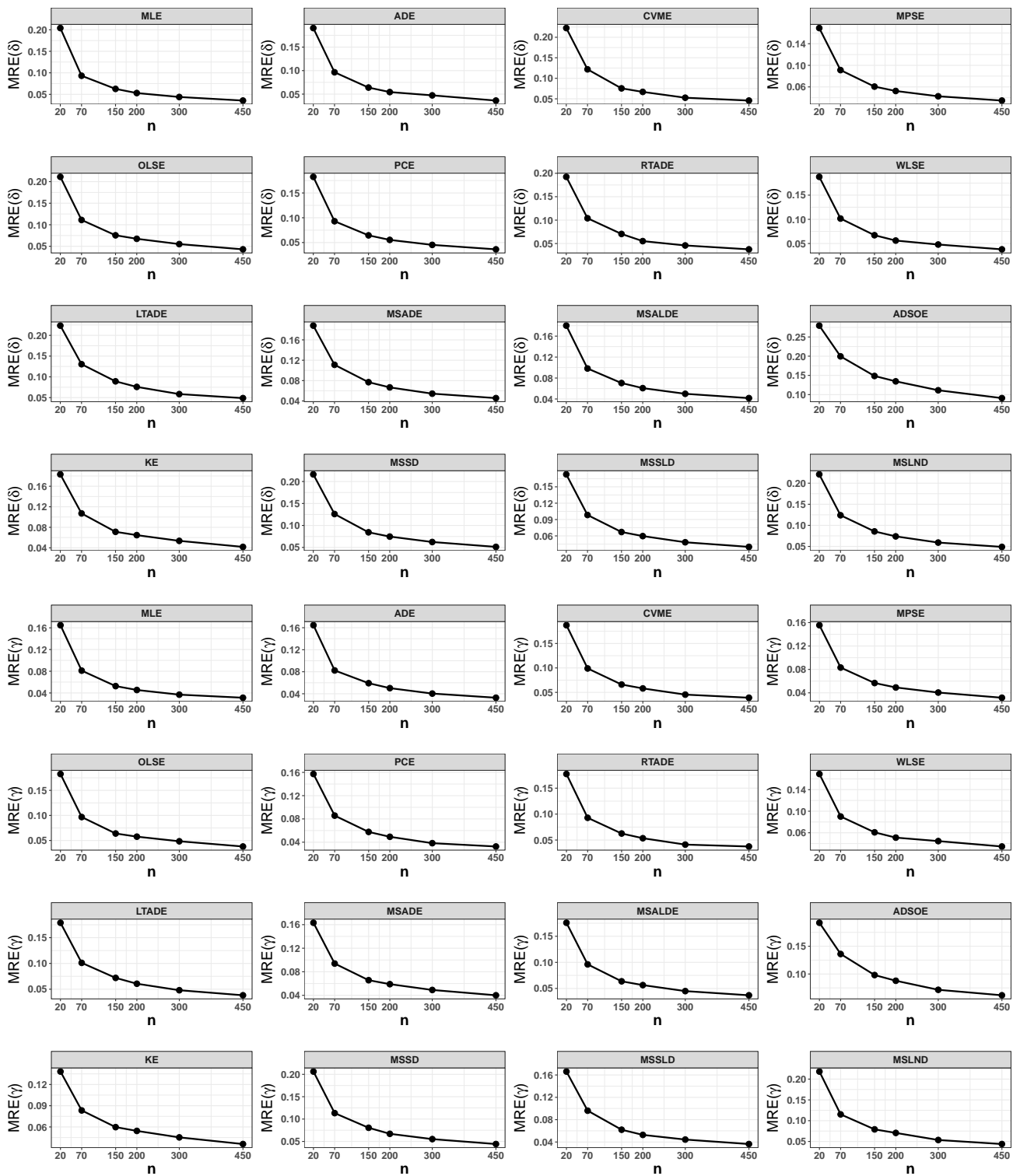


Figure 5. Graphical representation for MSE values presented in Table 6.





**Figure 6.** Graphical representation for MRE values presented in Table 6.

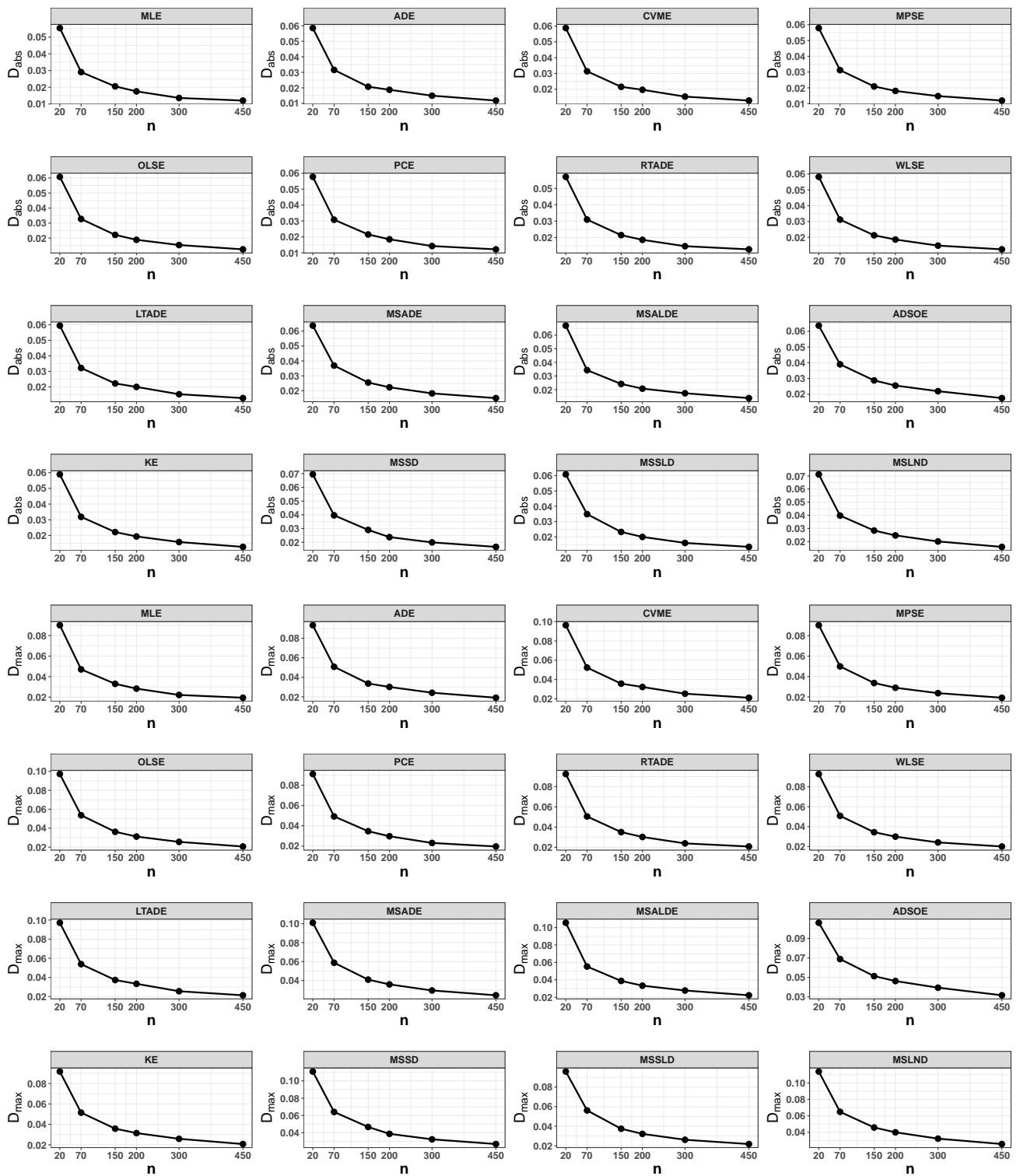


Figure 7. Graphical representation for  $D_{abs}$  and  $D_{max}$  values presented in Table 6.

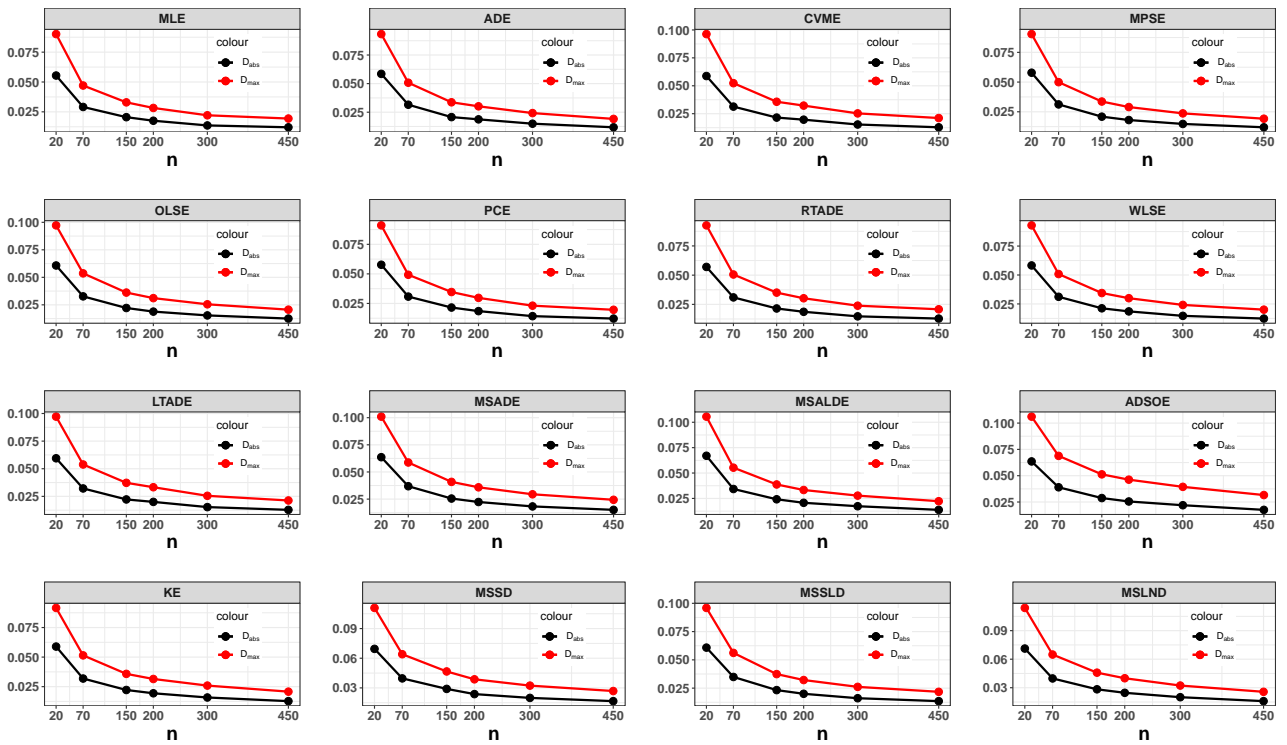


Figure 8. Comparison between  $D_{abs}$  and  $D_{max}$  values presented in Table 6.

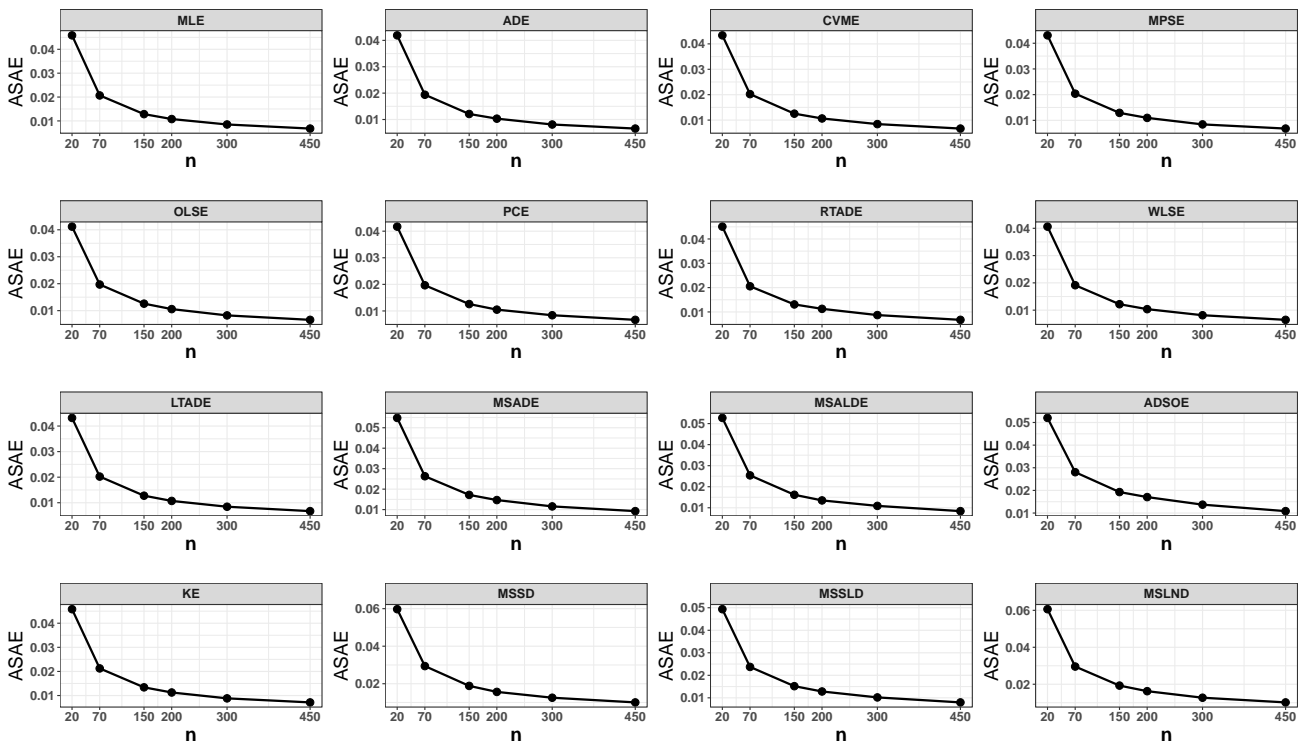


Figure 9. Graphical representation for ASAE values presented in Table 6.

## 6. Illustration with real data

To demonstrate the effectiveness of the proposed model, we have utilized two real-world datasets, one from agriculture and the other from medical sciences. The subsequent evaluation, application, and analysis of our model are detailed below. For the purpose of comparing our model, we selected several existing models that share similar characteristics and use HLD base function. The models chosen for this comparison include:

- The exponentiated generalized standard HLD (EGSHLD), developed by Cordeiro et al. [40].
- The exponentiated HLD, proposed by Seo and Kang [41].
- The Poisson generalized HLD (PGHLD), introduced by Muhammad and Liu [42].
- The Kumaraswamy HLD (KHLD), formulated by Usman et al. [43].
- The Type-II half logistic Weibull distribution (HLWD), created by Hassan et al. [28].
- The PHLD, developed by Krishnarani [23].

These models were selected for their relevance and compatibility with the HLD base function framework, providing a robust basis for comparison with our proposed model.

### First data:

This dataset discusses the total milk production in the first birth of 107 cows from the SINDI race [44]. These cows are property of the Carnuba farm, which belongs to the Agropecuaria Manoel Dantas Ltda (AMDA), located in Taperoa City, Paraiba (Brazil).

0.4365, 0.4260, 0.5140, 0.6907, 0.7471, 0.2605, 0.6196, 0.8781, 0.4990, 0.6058, 0.6891, 0.5770, 0.5394, 0.1479, 0.2356, 0.6012, 0.1525, 0.5483, 0.6927, 0.7261, 0.3323, 0.0671, 0.2361, 0.4800, 0.5707, 0.7131, 0.5853, 0.6768, 0.5350, 0.4151, 0.6789, 0.4576, 0.3259, 0.2303, 0.7687, 0.4371, 0.3383, 0.6114, 0.3480, 0.4564, 0.7804, 0.3406, 0.4823, 0.5912, 0.5744, 0.5481, 0.1131, 0.7290, 0.0168, 0.5529, 0.4530, 0.3891, 0.4752, 0.3134, 0.3175, 0.1167, 0.6750, 0.5113, 0.5447, 0.4143, 0.5627, 0.5150, 0.0776, 0.3945, 0.4553, 0.4470, 0.5285, 0.5232, 0.6465, 0.0650, 0.8492, 0.8147, 0.3627, 0.3906, 0.4438, 0.4612, 0.3188, 0.2160, 0.6707, 0.6220, 0.5629, 0.4675, 0.6844, 0.3413, 0.4332, 0.0854, 0.3821, 0.4694, 0.3635, 0.4111, 0.5349, 0.3751, 0.1546, 0.4517, 0.2681, 0.4049, 0.5553, 0.5878, 0.4741, 0.3598, 0.7629, 0.5941, 0.6174, 0.6860, 0.0609, 0.6488, 0.2747

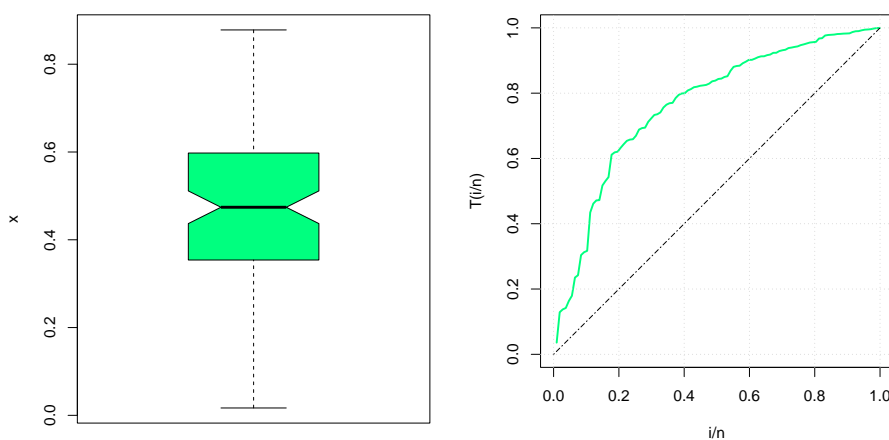


**Figure 10.** Box and TTT plots of first data.

We applied basic exploratory data analysis techniques to examine the dataset under study, with the results displayed in Figure 10. The left side shows a box plot, while the right side presents a total-time-on-test (TTT) plot. From the box plot, we observed that the data is approximately normally distributed. To understand the nature of the hazard function, we used the TTT plot as described by Aarset [45]. The TTT plot reveals a concave curve, indicating that the hazard function is increasing.

**Table 2.** MLEs with their SE of the first data.

Model	Parameter	SE	Parameter	SE	Parameter	SE
SPHLD( $\delta, \gamma$ )	3.7870	0.4370	2.2162	0.1836	–	–
EGSHLD( $\alpha, \beta$ )	7.0611	0.5863	3.3169	0.4593	–	–
EHL( $\lambda, \theta$ )	4.7771	0.3748	2.7077	0.3918	–	–
PGHLD( $\alpha, \beta, \delta$ )	0.5901	0.0916	2.6059	0.2187	133.3208	3.0465
KHLD( $\alpha, \beta, \theta$ )	2.5987	0.2161	141.1152	2.1935	0.5731	0.0893
HLWD( $\beta, \theta, \delta$ )	9.2668	0.0013	7.7567	0.0075	0.2865	0.0236
PHLD( $\delta, \gamma$ )	6.3117	0.7676	2.2754	0.1877	–	–

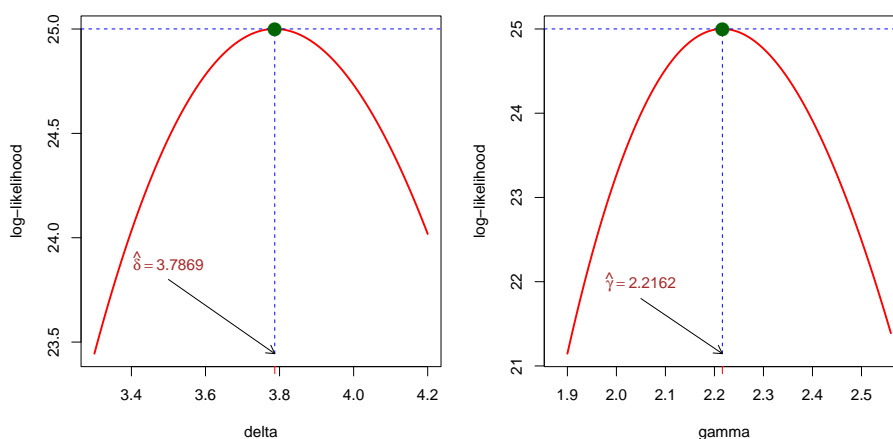


**Figure 11.** Profile log-likelihood plots of  $\delta$  and  $\gamma$  first data.

**Table 3.** Model adequacy and goodness of fit test statistics for the first data.

Models	-2logL	AIC	BIC	CAIC	HQIC	KS	p(KS)	CVM	p(CVM)	AD	p(AD)
SPHLD	-50.0009	-46.0009	-40.6552	-45.8877	-43.8338	0.0635	0.7812	0.1027	0.5727	0.8752	0.4295
EGSHLD	-18.5522	-14.5522	-9.2065	-14.439	-12.3851	0.1367	0.0367	0.678	0.0142	3.9479	0.0093
EHL	-20.661	-16.661	-11.3154	-16.5478	-14.494	0.1291	0.0566	0.6068	0.0213	3.6361	0.0132
PGHLD	-41.7841	-35.7841	-27.7656	-35.5556	-32.5335	0.0868	0.3958	0.2084	0.2519	1.5726	0.1601
KHLD	-42.0805	-36.0805	-28.062	-35.8519	-32.8299	0.0865	0.4001	0.2067	0.255	1.5561	0.1637
HLWD	-50.7479	-44.7479	-36.7294	-44.5193	-41.4973	0.083	0.4532	0.1787	0.3131	1.088	0.3141
PHLD	-48.4568	-44.4568	-39.1112	-44.3436	-42.2898	0.0647	0.7624	0.1082	0.5469	0.9613	0.378

### Second data:

The data presented by [46], characterized by right-skewness, represents the survival times of 121 breast cancer patients treated at a tertiary care center between 1929 and 1938.

”0.3, 0.3, 4.0, 5.0, 5.6, 6.2, 6.3, 6.6, 6.8, 7.4, 7.5, 8.4, 8.4, 10.3, 11.0, 11.8, 12.2, 12.3, 13.5, 14.4, 14.4, 14.8, 15.5, 15.7, 16.2, 16.3, 16.5, 16.8, 17.2, 17.3, 17.5, 17.9, 19.8, 20.4, 20.9, 21.0, 21.0, 21.1, 23.0, 23.4, 23.6, 24.0, 24.0, 27.9, 28.2, 29.1, 30.0, 31.0, 31.0, 32.0, 35.0, 35.0, 37.0, 37.0, 37.0, 38.0, 38.0,

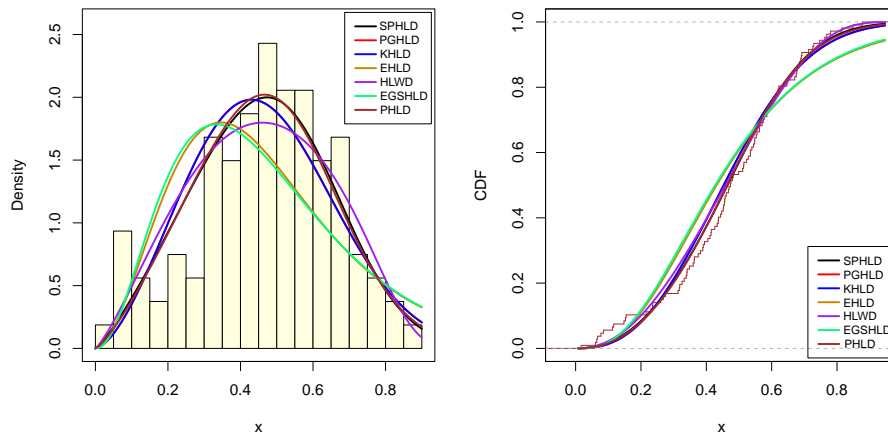


**Figure 12.** PDF and CDF plots of the models under comparison of the first data.

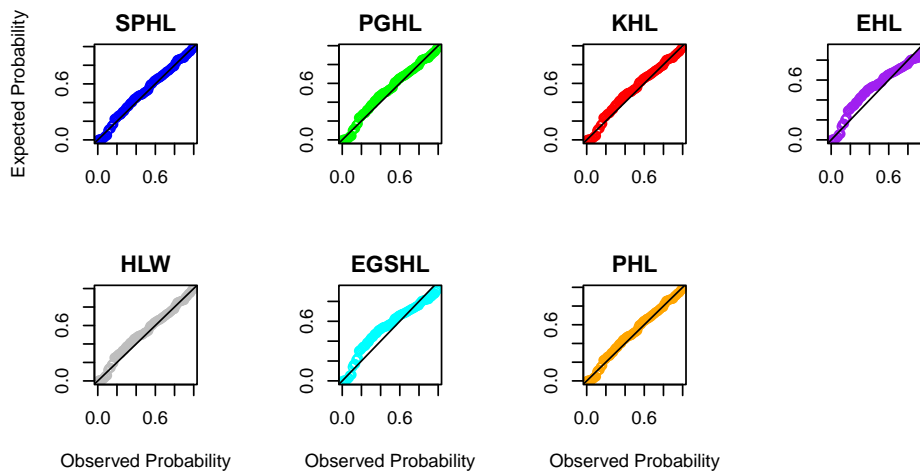


**Figure 13.** PP plots of the models under comparison of the first data.

38.0, 39.0, 39.0, 40.0, 40.0, 40.0, 41.0, 41.0, 41.0, 42.0, 43.0, 43.0, 43.0, 44.0, 45.0, 45.0, 46.0, 46.0, 47.0, 48.0, 49.0, 51.0, 51.0, 51.0, 52.0, 54.0, 55.0, 56.0, 57.0, 58.0, 59.0, 60.0, 60.0, 60.0, 61.0, 62.0, 65.0, 65.0, 67.0, 67.0, 68.0, 69.0, 78.0, 80.0, 83.0, 88.0, 89.0, 90.0, 93.0, 96.0, 103.0, 105.0, 109.0, 109.0, 111.0, 115.0, 117.0, 125.0, 126.0, 127.0, 129.0, 129.0, 139.0, 154.0”

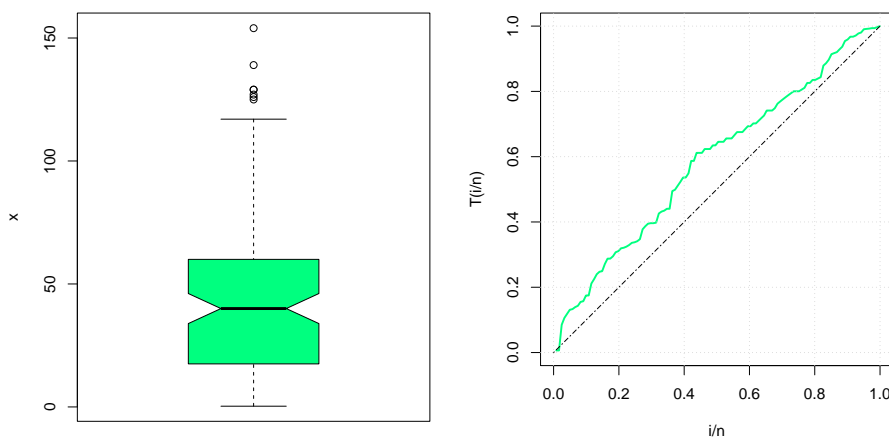


**Figure 14.** Box and TTT plots of second data.

Similarly, the results are presented in Figure 14 for the second dataset. A box plot is displayed on the left, and on the right, a TTT plot is shown. The box plot indicates that the data is right-skewed along with some outliers. The TTT plot reveals a concave curve, indicating that the hazard function is increasing.

**Table 4.** MLEs with their SE of the second data.

Model	parameter	SE	parameter	SE	parameter	SE
SPHLD( $\delta, \gamma$ )	0.0134	0.0048	1.0754	0.0806	–	–
EGSHLD( $\alpha, \beta$ )	0.0271	0.0029	1.4176	0.1774	–	–
EHL( $\lambda, \theta$ )	0.0330	0.0030	1.1827	0.1406	–	–
PGHLD( $\alpha, \beta, \delta$ )	0.0029	6.0E-04	1.3095	0.0959	31.6416	3.0606
KHLD( $\alpha, \beta, \theta$ )	1.7763	2.0E-04	0.1171	0.0106	0.2100	1.0E-04
HLWD( $\beta, \theta, \delta$ )	3.2E-05	0.0000	2.3012	0.0925	0.5459	0.0382
PHLD( $\delta, \gamma$ )	0.0188	0.0068	1.1120	0.0833	–	–

**Table 5.** Model adequacy and goodness of fit test statistics for the second data.

Models	-2logL	AIC	BIC	CAIC	HQIC	KS	p(KS)	CVM	p(CVM)	AD	p(AD)
SPHLD	1158.5700	1162.5700	1168.1620	1162.4700	1164.8410	0.0460	0.9603	0.0697	0.7543	0.5285	0.7176
EGSHLD	1161.6180	1165.6180	1171.2090	1165.7180	1167.8890	0.0848	0.3489	0.0784	0.7023	0.5126	0.7337
EHL	1158.7411	1162.7411	1168.4002	1162.5110	1164.9820	0.0569	0.8286	0.0519	0.8652	0.4096	0.8389
PGHLD	1158.6990	1164.1990	1172.5860	1164.4010	1167.6050	0.0606	0.7658	0.0522	0.8638	0.3987	0.8498
KHLD	1163.9130	1169.9130	1178.3000	1170.1140	1173.3190	0.1032	0.1521	0.1349	0.4395	0.7670	0.5051
HLWD	1158.8090	1163.0090	1171.3960	1163.2110	1166.4150	0.0538	0.8752	0.0634	0.7934	0.4578	0.7898
PHLD	1158.6310	1162.6310	1168.8022	1162.5310	1164.8702	0.0492	0.9311	0.0597	0.8170	0.4685	0.7788

The parameters ( $\delta, \gamma$ ) of the proposed distribution are estimated using the ML method, implemented through the ‘maxLik’ package as described by Henningsen and Toomet [47]. This estimation is performed using R programming software [48], with further details available in Lambert [49]. The afore-

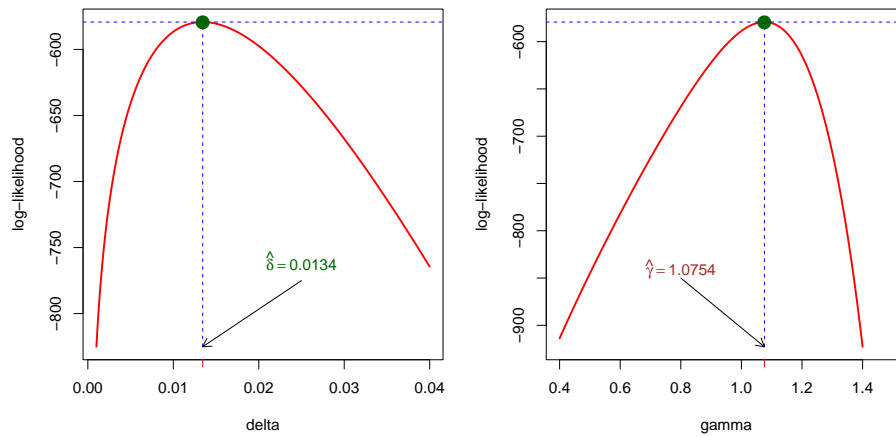


**Figure 15.** Profile log-likelihood plots of  $\delta$  and  $\gamma$  second data.

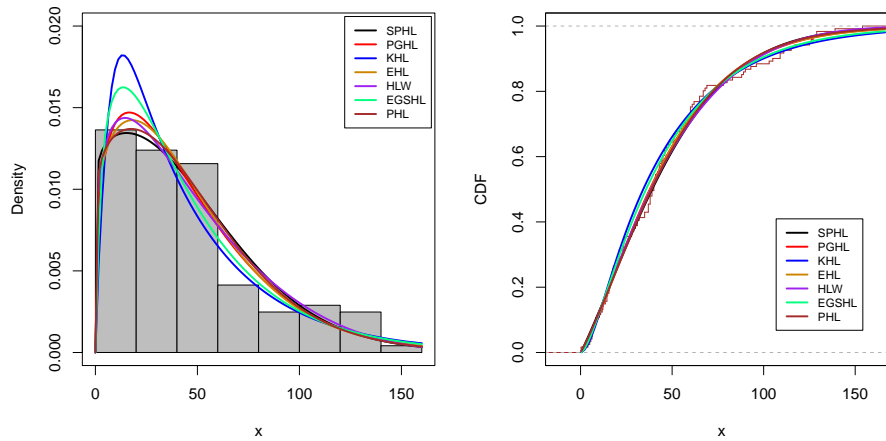


**Figure 16.** PDF and CDF plots of the models under comparison of the second data.

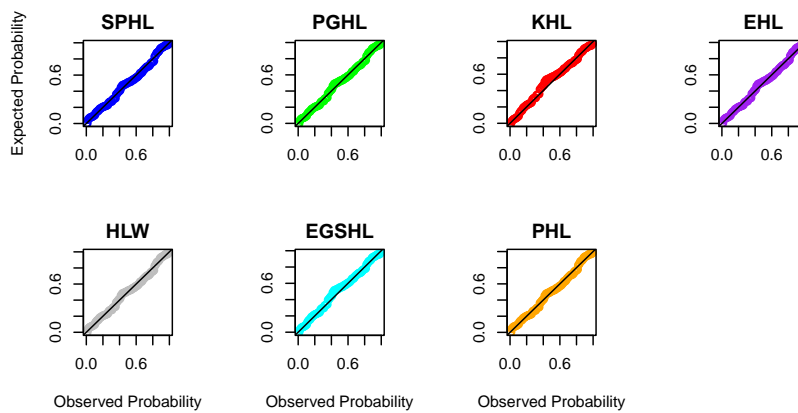


**Figure 17.** PP plots of the models under comparison of the second data.



mentioned candidate distributions and the SPHLD also fit the studied datasets. The MLEs and their corresponding standard errors (SEs) are calculated, with the results presented in Tables 2 and 4, respectively. We have also displayed the profile log-likelihood plots for both parameters of the proposed model in Figures 11 and 15, respectively, for both datasets. These plots indicate that the parameter estimation through the ML method is unique and consistent. PP plots of the models under comparison of the first and second datasets are presented in Figures 13 and 17.

### Model Selection

To determine the best model among the candidates, we used several standard criteria: log-likelihood ( $-2 \log L$ ), Akaike's information criterion (AIC), Bayesian information criterion (BIC), corrected AIC (CAIC), Hannan-Quinn information criterion (HQIC) and goodness-of-fit test statistics, including the Kolmogorov-Smirnov (KS) test, AD test, and CVM test. The corresponding p-values for these tests are denoted as  $p(KS)$ ,  $p(AD)$ , and  $p(CVM)$ , respectively. The best model is identified by the smallest values of ( $-2 \log L$ ), AIC, BIC, CAIC, HQIC, KS, AD, and CVM, and the largest p-values, as recommended by Burnham and Anderson [50].

The results in Tables 3 and 5 show that the proposed SPHLD outperforms the other candidate models. This conclusion is further supported by the graphical representations of the fitted PDF and CDF shown in Figures 12 and 16, where the SPHLD provides the best fit for the data.

### Model Validation

We calculated the KS distances between the fitted distribution function and the empirical distribution function for both datasets to evaluate the model's validity. The KS distances are 0.0635 and 0.0460, with corresponding p-values of 0.7812 and 0.9603, respectively. These calculations used the parameters estimated by the ML method. The results indicate that the SPHLD fits the data very well (see other metrics AD and CVM also in Tables 3 and 5).

## 7. Concluding remarks

This work provides a significant contribution to the creation of a flexible trigonometric extension of the PHL. In particular, we use properties from the sine-generated family of distributions to create a novel two-parameter lifespan model, called the SPHLD. The primary reason behind this is that asymmetric datasets may make the new distribution more useful for simulating lifespan phenomena. The distribution takes on a number of asymmetric form configurations, as seen by the density function graphs of the SPHLD. In addition, the hazard rate graphs of the SPHLD showed both monotonic rises and declines. Statistical properties of the SPHLD that are computed include the quantile function, moments, central moments, incomplete moments, and stress-strength reliability. The SPHLD parameters are estimated using several different classical estimating methods. To assess the consistency of the various estimates and identify the most accurate estimating strategy, a simulation study was conducted based on a few accuracy metrics. The SPHLD outperforms several other distributions, according to analyses of actual data. Simulation analysis consistently demonstrated that the maximum product spacing exhibited the highest accuracy among the selected estimation techniques, followed by the maximum likelihood method, making it the preferred method for parameter estimation. The current study's primary limitation is its only focus on traditional estimating techniques for model parameters, which depend on complete sample data. Future studies can examine both Bayesian and traditional parameter estimation methods, with an emphasis on how they could be used in ranked set sampling.











**Table 11.** Partial and overall ranks for all estimation methods of our proposed model.

Parameter	$n$	MLE	ADE	CVME	MPSE	OLSE	PCE	RTADE	WLSE	LTADE	MSADE	MSALDE	ADSOE	KE	MSSD	MSSLD	MSLND
$\delta = 2.5, \gamma = 4.0$	20	7.0	6.0	13.0	1.0	11.0	2.0	9.0	4.5	12.0	8.0	10.0	15.0	3.0	14.0	4.5	16.0
	70	1.0	4.0	11.0	2.0	10.0	3.0	6.0	5.0	13.0	12.0	8.5	16.0	7.0	14.0	8.5	15.0
	150	1.0	3.0	9.0	2.0	11.0	4.0	6.0	5.0	13.0	12.0	10.0	16.0	8.0	15.0	7.0	14.0
	200	1.0	4.0	11.0	2.0	9.0	3.0	6.0	5.0	13.0	12.0	10.0	16.0	8.0	14.0	7.0	15.0
	300	1.0	4.0	8.0	3.0	11.0	2.0	5.0	6.0	12.0	13.0	9.0	16.0	10.0	15.0	7.0	14.0
	450	2.0	3.0	11.0	1.0	9.0	4.0	6.0	5.0	12.0	13.0	10.0	16.0	7.0	15.0	8.0	14.0
$\delta = 0.8, \gamma = 0.3$	20	2.0	3.0	9.0	1.0	7.0	15.0	5.0	4.0	10.0	11.0	8.0	16.0	12.0	14.0	6.0	13.0
	70	4.0	2.0	8.5	5.0	7.0	15.0	3.0	1.0	8.5	12.0	10.0	16.0	11.0	13.0	6.0	14.0
	150	1.0	3.0	7.0	2.0	8.0	14.5	4.0	5.0	10.0	12.0	9.0	16.0	11.0	13.0	6.0	14.5
	200	3.0	1.0	7.0	4.0	6.0	15.0	5.0	2.0	10.0	12.0	9.0	16.0	11.0	13.0	8.0	14.0
	300	1.0	3.0	7.0	2.0	6.0	16.0	4.0	5.0	9.0	12.0	10.0	15.0	11.0	14.0	8.0	13.0
	450	3.0	2.0	6.0	1.0	7.0	16.0	5.0	4.0	11.0	12.0	10.0	15.0	8.0	13.0	9.0	14.0
$\delta = 0.4, \gamma = 1.5$	20	3.0	1.5	12.0	5.0	8.5	4.0	8.5	6.0	10.0	11.0	13.0	14.0	1.5	15.0	7.0	16.0
	70	1.0	4.0	10.0	5.5	8.0	5.5	7.0	2.0	11.0	13.0	12.0	14.0	3.0	15.0	9.0	16.0
	150	1.0	5.0	10.0	2.0	8.0	4.0	7.0	6.0	9.0	14.0	12.0	13.0	3.0	15.0	11.0	16.0
	200	1.0	5.0	10.0	3.0	8.0	6.0	9.0	4.0	7.0	14.0	11.0	13.0	2.0	15.0	12.0	16.0
	300	3.0	5.0	9.5	1.0	8.0	6.0	7.0	2.0	9.5	14.0	13.0	12.0	4.0	15.0	11.0	16.0
	450	2.0	6.0	11.0	1.0	7.5	3.0	9.0	4.0	7.5	14.0	13.0	12.0	5.0	16.0	10.0	15.0
$\delta = 2.0, \gamma = 0.75$	20	7.0	4.0	12.0	1.0	11.0	9.5	6.0	5.0	13.0	9.5	8.0	15.0	2.0	14.0	3.0	16.0
	70	2.0	7.0	10.0	1.0	8.5	11.0	5.5	4.0	13.0	12.0	8.5	16.0	3.0	14.0	5.5	15.0
	150	1.0	5.0	10.0	2.0	8.5	11.0	7.0	3.0	13.0	12.0	8.5	16.0	4.0	15.0	6.0	14.0
	200	1.0	3.0	10.0	2.0	8.0	12.0	5.0	7.0	11.0	13.0	9.0	16.0	4.0	14.0	6.0	15.0
	300	1.0	5.0	10.0	2.0	8.0	11.0	3.0	4.0	12.0	13.0	9.0	16.0	6.0	15.0	7.0	14.0
	450	1.0	5.0	10.0	2.0	8.0	12.0	4.0	3.0	11.0	13.0	9.0	16.0	6.0	15.0	7.0	14.0
$\delta = 3.5, \gamma = 0.5$	20	4.5	3.0	9.0	2.0	12.0	10.0	8.0	4.5	13.0	7.0	11.0	14.0	1.0	15.0	6.0	16.0
	70	3.0	4.0	11.0	2.0	10.0	15.0	5.0	6.5	12.0	8.0	9.0	16.0	1.0	14.0	6.5	13.0
	150	3.0	5.0	10.0	1.0	9.0	15.0	6.0	4.0	12.0	11.0	8.0	16.0	2.0	13.0	7.0	14.0
	200	3.0	5.0	11.0	2.0	8.0	15.0	6.0	4.0	12.0	10.0	9.0	16.0	1.0	14.0	7.0	13.0
	300	2.5	4.0	10.0	2.5	8.0	15.0	6.0	5.0	12.0	11.0	9.0	16.0	1.0	13.0	7.0	14.0
	450	2.0	5.0	10.0	4.0	9.0	15.0	6.0	3.0	12.0	11.0	8.0	16.0	1.0	14.0	7.0	13.0
$\sum$ Ranks	69.0	119.5	293.0	67.0	258.0	289.5	179.0	128.5	333.5	351.5	293.5	456.0	157.5	428.0	220.0	436.5	
Overall Rank	2	3	10	1	8	9	6	4	12	13	11	16	5	14	7	15	

## Use of AI tools declaration

The authors declare they have not used Artificial Intelligence (AI) tools in the creation of this article.

## Acknowledgments

This research is supported by researchers Supporting Project number (RSPD2025R548), King Saud University, Riyadh, Saudi Arabia.

## Conflict of interest

The authors declare there are no conflicts of interest.

## References

1. A. Marshall, I. Olkin, A new method for adding a parameter to a family of distributions with applications to the exponential and Weibull families, *Biometrika*, **84** (1997), 641–652. <https://doi.org/10.1093/biomet/84.3.641>
2. N. Eugene, C. Lee, F. Famoye, Beta-normal distribution and its applications, *Commun. Stat.-Theory Methods*, **31** (2002), 497–512. <https://doi.org/10.1081/STA-120003130>
3. A. Alzaatreh, F. Famoye, C. Lee, A new method for generating families of continuous distributions, *Metron*, **71** (2013), 63–79. <https://doi.org/10.1007/s40300-013-0007-y>
4. A. Al-Shomrani, O. Arif, A. Shawky, S. Hanif, M. Q. Shahbaz, Topp-Leone family of distributions: Some properties and application, *Pak. J. Stat. Oper. Res.*, **12** (2016), 443–451. <https://doi.org/10.18187/pjsor.v12i3.1458>
5. A. S. Hassan, E. A. El-Sherpieny, S. A. El-Taweel, New Topp Leone-G family with mathematical properties and applications, *J. Phys.: Conf. Ser.*, **12** (2021). <https://doi.org/10.1088/1742-6596/1860/1/012011>.
6. M. A. Badr, I. Elbatal, F. Jamal, C. Chesneau, M. Elgarhy, The transmuted odd Fréchet-G family of distributions: Theory and applications, *Mathematics*, **8** (2020), 958. <https://doi.org/10.3390/math8060958>
7. M. Aslam, Z. Asghar, Z. Hussain, S. F. Shah, A modified T-X family of distributions: Classical and Bayesian analysis, *J. Taibah Univ. Sci.*, **14** (2020), 254–264. <https://doi.org/10.1080/16583655.2020.1732642>
8. A. S. Hassan, M. A. H. Sabry, A. M. Elsehtery, A new probability distribution family arising from truncated power Lomax distribution with application to Weibull model, *Pak. J. Stat. Oper. Res.*, **16** (2020), 661–674. <https://doi.org/10.1007/s12015-020-09979-4>
9. F. S. Gomes-Silva, A. Percontini, E. de Brito, M. W. Ramos, R. Venâncio, G. M. Cordeiro, The odd Lindley-G family of distributions, *Austrian J. Stat.*, **46** (2017), 65–87. <https://doi.org/10.17713/ajs.v46i1.222>
10. A. S. Hassan, S. G. Nassar, Power Lindley-G family of distributions, *Ann. Data Sci.*, **6** (2019), 189–210. <https://doi.org/10.1007/s40745-018-0159-y>



11. I. Elbatal, N. Alotaibi, E. M. Almetwally, S. A. Alyami, M. Elgarhy, On odd perks-G class of distributions: properties, regression model, discretization, Bayesian and non-Bayesian estimation, and applications, *Symmetry*, **14** (2022), 883. <https://doi.org/10.3390/sym14050883>
12. A. Z. Afify, G. M. Cordeiro, N. A. Ibrahim, J. M. Elgarhy, M. A. Nasir, The Marshall-Olkin odd Burr III-G family: Theory, estimation, and engineering applications, *IEEE Access*, **9** (2021), 4376–4387. <https://doi.org/10.1109/ACCESS.2020.3044156>
13. C. Chesneau, T. E. Achi, Modified odd Weibull family of distributions: Properties and applications, *J. Indian Soc. Probab. Stat.*, **21** (2020), 259–286. <https://doi.org/10.1007/s41096-020-00075-x>
14. J. T. Eghwerido, D. J. Ikwuoché, O. D. AdubisiM, Inverse odd Weibull generated family of distribution, *Pak. J. Stat. Oper. Res.*, **16** (2020), 617–633.
15. D. Kumar, U. Singh, S. K. Singh, A new distribution using sine function- its application to bladder cancer patients data, *J. Stat. Appl. Probab.*, **4** (2015), 417–427.
16. Z. Mahmood, C. Chesneau, M.H. Tahir, A new sine-G family of distributions: properties and applications, *Bull. Comput. Appl. Math.*, **7** (2019), 53–81.
17. N. Balakrishnan, Order statistics from the half logistic distribution. *J. Stat. Comput. Simul.*, **20** (1985), 287–309.
18. R. S. Rao, P. L. Mamidi, R. R. Kantam, Modified maximum likelihood estimation: Inverse half logistic distribution, *J. Math.*, **5** (2016), 11–19.
19. H. Torabi, F. L. Bagheri, Estimation of parameters for an extended generalized half logistic distribution based on complete and censored data, *J. Iranian Stat. Soc.*, **9** (2010), 171–195.
20. G. M. Cordeiro, M. Alizadeh, E. M. M. Ortega, The exponentiated half logistic family of distributions: properties and applications, *J. Probab. Stat.*, **2014** (2014), 864396. <https://doi.org/10.1155/2014/864396>
21. J. Oliveira, J. Santos, C. Xavier, D. Trindade, G. M. Cordeiro, The McDonald half-logistic distribution: theory and practice, *Commun. Stat. Theory Methods*, **45** (2016), 2005–2022. <https://doi.org/10.1080/03610926.2013.873131>
22. A. H. Hassan, M. Elgarhy, M. Shakil, Type II half logistic family of distributions with applications, *Pak. J. Stat. Oper. Res.*, **13** (2017), 245–264. <https://doi.org/10.18187/pjsor.v13i2.1560>
23. S. D. Krishnarani, On a power transformation of half-logistic distribution, *J. Probab. Stat.*, **20** (2016), 1–10.
24. R. M. Usman, A. M. Haq, J. Talib, Kumaraswamy half-logistic distribution: properties and applications, *J. Stat. Appl. Probab.*, **6** (2017), 597–609. <https://doi.org/10.18576/jsap/060315>
25. D. Yegen, G. Ozel, Marshall-Olkin half logistic distribution with theory and applications, *Alphanum. J.*, **6** (2018), 408–416. <https://doi.org/10.17093/alphanumeric.409992>
26. M. Elgarhy, A. S. Hassan, S. Fayomi, Maximum likelihood and Bayesian estimation for two-parameter type I half logistic Lindley distribution, *J. Comput. Theor. Nanosci.*, **15** (2018), 1–9. <https://doi.org/10.1166/jctn.2018.7600>
27. A. F. Samuel, O. A. Kehinde, A study on transmuted half logistic distribution: Properties and application, *Int. J. Stat. Distribut. Appl.*, **5** (2019), 54–59.

28. A. S. Hassan, M. Elgarhy, M. A. Haq, S. Alrajhi, On type II half logistic Weibull distribution with applications, *Math. Theory Model.*, **19**(2019), 49–63. <https://doi.org/10.21608/esju.2019.268726>
29. M. Anwar, A. Bibi, The half-logistic generalized Weibull distribution, *J. Probab. Stat.*, (2018), 8767826. <https://doi.org/10.1155/2018/8767826>
30. A. Algarni, A. M. Almarashi, I. Elbatal, A. S. Hassan, E. M. Almetwally, A. M. Daghistani, et al., Type I half logistic Burr X-G family: Properties, Bayesian, and non-Bayesian estimation under censored samples and applications to COVID-19 data, *Math. Probl. Eng.*, **2021**, (2021), 5461130. <https://doi.org/10.1155/2021/5461130>
31. G. S. Mohammad, A new two-parameter modified half-logistic distribution: Properties and Applications, *Stat. Optim. Inf. Comput.*, **10** (2022), 589–605. <https://doi.org/10.19139/soic-2310-5070-1210>
32. A. S. Hassan, A. Fayomi, A. Algarni, E. M. Almetwally, Bayesian and non-Bayesian inference for unit-exponentiated half-logistic distribution with data analysis, *Appl. Sci.*, **12** (2022), 11253. <https://doi.org/10.3390/app122111253>
33. H. Majid, An extended type I half-logistic family of distributions: Properties, applications and different method of estimations, *Math. Slovaca*, **72** (2022), 745–764. <https://doi.org/10.1515/ms-2022-0051>
34. R. M. I. Arshad, M. H. Tahir, C. Chesneau, S. Khan, F. Jamal, The gamma power half-logistic distribution: theory and applications, *Sao Paulo J. Math. Sci.*, **17** (2023), 1142–1169. <https://doi.org/10.1007/s40863-022-00331-x>
35. S. M. Alghamdi, M. Shrahili, A. S. Hassan, A. M. Gemeay, I. Elbatal, M. Elgarhy, Statistical inference of the half logistic modified Kies exponential model with modeling to engineering data, *Symmetry*, **15** (2023), 586. <https://doi.org/10.3390/sym15030586>
36. O. D. Adubisi, C. E. Adubisi, Novel distribution for modeling uncensored and censored survival time data and regression model, *Reliab. Theory Appl.*, **3** (2023), 808–824.
37. R. C. H. Cheng, N. A. K. Amin, Maximum product-of-spacings estimation with applications to the log-normal distribution, *University of Wales IST, Math Report*, (1979), 79–103.
38. R. C. H. Cheng, N. A. K. Amin, Estimating parameters in continuous univariate distributions with a shifted origin, *J. R. Stat. Soc.: Ser. B (Methodol.)* **45** (1983), 394–403. <https://doi.org/10.1111/j.2517-6161.1983.tb01268.x>
39. B. Ranney, The maximum spacing method: An estimation method related to the maximum likelihood method, *Scand. J. Stat.*, **11** (1984), 93–112.
40. G. M. Cordeiro, T. A. de Andrade, M. Bourguignon, F. G. Silva, The exponentiated generalized standardized half-logistic distribution, *Int. J. Stat. Probab.*, **6** (2017), 24–42. <https://doi.org/10.5539/ijsp.v6n3p24>
41. J. I. Seo, S. B. Kang, Notes on the exponentiated half logistic distribution, *Appl. Math. Model.*, **39** (2015), 6491–6500.
42. M. Muhammad, L. Liu, A new extension of the generalized half logistic distribution with applications to real data, *Entropy*, **21** (2019), 339. <https://doi.org/10.3390/e21040339>

43. R. M. Usman, M. Haq, J. Talib, Kumaraswamy half-logistic distribution: properties and applications, *J. Stat. Appl. Probab.*, **6** (2017), 597–609. <https://doi.org/10.18576/jsap/060315>
44. G. M. Cordeiro, R. B. dos Santos, The beta power distribution. *Brazil J. Probab. Stat.*, **26** (2012), 88–112. <https://doi.org/10.1214/10-BJPS124>
45. M. V. Aarset, How to identify a bathtub hazard rate, *IEEE Trans. Reliab.*, **36** (1987), 106–108. <https://doi.org/10.1109/TR.1987.5222310>
46. E. T. Lee, Statistical methods for survival data analysis, *IEEE Trans. Reliab.*, **35** (1986), 123–123. <https://doi.org/10.1109/TR.1986.4335370>
47. A. Henningsen, O. Toomet, maxLik: A package for maximum likelihood estimation in R, *Comput. Stat.*, **26** (2011), 443–458. <https://doi.org/10.1007/s00180-010-0217-1>
48. R Core Team, R: A language and environment for statistical computing, Foundation for Statistical Computing, Vienna, Austria, 2013.
49. B. Lambert, A student's guide to Bayesian statistics, in *A Student's Guide to Bayesian Statistics*, (2018), 1–520.
50. K. P. Burnham, D. R. Anderson, Model selection and multimodel inference: a practical information-theoretic approach, *Springer*, 2002.



AIMS Press

© 2025 the Author(s), licensee AIMS Press. This is an open access article distributed under the terms of the Creative Commons Attribution License (<https://creativecommons.org/licenses/by/4.0>)